Forever alone? Testing single eccentric planetary systems for multiple companions

Robert A. Wittenmyer[1], Songhu Wang[2], Jonathan Horner[1], C.G. Tinney[1], R.P. Butler[3], H.R.A. Jones[4], S.J. O'Toole[5], J. Bailey[1], B.D. Carter[6], G.S. Salter[1], D. Wright[1], Ji-Lin Zhou[2]

`rob@phys.unsw.edu.au`

ABSTRACT

Determining the orbital eccentricity of an extrasolar planet is critically important for understanding the system's dynamical environment and history. However, eccentricity is often poorly determined or entirely mischaracterized due to poor observational sampling, low signal-to-noise, and/or degeneracies with other planetary signals. Some systems previously thought to contain a single, moderate-eccentricity planet have been shown, after further monitoring, to host two planets on nearly-circular orbits. We investigate published apparent single-planet systems to see if the available data can be better fit by two lower-eccentricity planets. We identify nine promising candidate systems and perform detailed dynamical tests to confirm the stability of the potential new multiple-planet systems. Finally, we compare the expected orbits of the single- and double-planet scenarios to better inform future observations of these interesting systems.

Subject headings: planetary systems – techniques: radial velocities

[1]Department of Astrophysics, School of Physics, Faculty of Science, The University of New South Wales, Sydney, NSW 2052, Australia

[2]Department of Astronomy & Key Laboratory of Modern Astronomy and Astrophysics in Ministry of Education, Nanjing University, Nanjing 210093, China.

[3]Department of Terrestrial Magnetism, Carnegie Institution of Washington, 5241 Broad Branch Road, NW, Washington, DC 20015-1305, USA

[4]University of Hertfordshire, Centre for Astrophysics Research, Science and Technology Research Institute, College Lane, AL10 9AB, Hatfield, UK

[5]Australian Astronomical Observatory, PO Box 915, North Ryde, NSW 1670, Australia

[6]Faculty of Sciences, University of Southern Queensland, Toowoomba, Queensland 4350, Australia

1. Introduction

The radial-velocity method remains the most versatile technique for determining the full orbital properties (e.g. minimum mass, eccentricity) of extrasolar planets. More than 500 planets have been discovered by this method, and considerable efforts are afoot to understand the true underlying distribution of planetary properties based on these data (Cumming et al. 2008; Shen & Turner 2008; O'Toole et al. 2009a,c; Howard et al. 2010b; Wittenmyer et al. 2010, 2011a,b). However, there are significant biases in the measurement of planetary parameters from sparsely sampled radial-velocity data, especially if the amplitude (K) of the signal is small. Particularly problematic is the orbital eccentricity, a quantity which is critically important for understanding the formation and dynamical history of planetary systems (Zhou et al. 2007; Ford & Rasio 2008; Shen & Turner 2008). Keplerian orbit-fitting algorithms, in a blind mathematical attempt to minimise χ^2, often resort to increasing the eccentricity of a model fit. Shen & Turner (2008) found this introduced bias toward higher fitted eccentricities to be most egregious for data with signal-to-noise ratio $K/\sigma \lesssim 3$. Similarly, O'Toole et al. (2009a) showed that there is a computational bias against fitting eccentricities near zero, and that the true uncertainties in orbital parameters can be 5-10 times larger than the formal uncertainties emerging from standard least-squares fits. There is, therefore, reason to suspect that the observed eccentricity distribution of radial-velocity detected exoplanets is biased towards higher eccentricities.

Recently, further radial-velocity monitoring has revealed additional planets in two systems previously thought to host a single planet (HD 142 and HD 159868: Wittenmyer et al. 2012b), and the best-fit eccentricities of the previously known planets have significantly decreased as a result of fitting *two* planetary signals. This was most obvious for HD 159868, where the previously known planet, with a period of ∼1180 days, had an orbit best fit with a very high $e = 0.69 \pm 0.02$ (O'Toole et al. 2007). As a result of new data, and a two-planet solution, HD 159868b is now best fit with a circular orbit ($e = 0.01\pm0.03$). The possibility that two nearly-circular orbits can masquerade as a single, eccentric orbit has been explored by Anglada-Escudé et al. (2010) and Rodigas & Hinz (2009). Motivated by these findings, we now ask "Which eccentric single-planet systems can be better fit with two low-eccentricity planets?"

The ambiguities in orbital eccentricity can arise from one of four degeneracies, which we summarise here. First, there is the degeneracy betweeen a single planet on an eccentric orbit and two planets on circular orbits in a 2:1 configuration (Anglada-Escudé et al. 2010). Second is the degeneracy between one eccentric planet and two co-orbital planets (i.e. in a 1:1 resonance or "Trojan pair"), as described in Laughlin & Chambers (2002) and Giuppone et al. (2012). Third is the degeneracy between a single eccentric planet and a

circular planet with a long-period companion (Rodigas & Hinz 2009). The fourth degeneracy is that noted above for HD 159868: that between a single eccentric planet and two nearly-circular planets with poorly sampled orbital periods (Wittenmyer et al. 2012b).

This paper is organised as follows: Section 2 describes the data and analysis procedures, Section 3 gives the results of our efforts to fit two low-eccentricity planets, and details those systems which had the most promising results. Finally, we discuss our conclusions in Section 4.

2. Data Analysis and Orbit Fitting

We selected all radial-velocity detected single-planet systems with publicly available data and published eccentricities $e > 0.3$. This can be considered a high-eccentricity subset, as the mean eccentricity for the current population of confirmed planets is 0.22[1]. The mean uncertainty on the published eccentricities is 0.05, though we note that the uncertainties arising from least-squares fit can be underestimated (O'Toole et al. 2009a). In addition, we excluded any transiting planets (e.g. HD 17156b and HD 80606b), because for these cases, the transit should be simultaneously fit with the radial velocities, a task which is beyond the scope of this paper. After applying these selection criteria, 82 stars remained. A summary of the data used here is given in Table 1. All previously unpublished AAT data used in this work are now given in the Appendix, Tables 4–15.

To facilitate the comparison of the two-planet models with the single eccentric-planet model, we first re-fit all available radial-velocity data with a single planet (with no restrictions on e). For those stars with data from multiple sources, this approach ensures consistent treatment by using the same fitting procedure for all stars. These results are referred to as Method 1 as given in Table 2. Then, for each system, we fit all available data using a genetic algorithm, which has proven useful in previous work where the system parameters are extremely uncertain or data are sparse (Horner et al. 2012b; Wittenmyer et al. 2012a, 2011c; Tinney et al. 2011b; Cochran et al. 2007). The genetic algorithm used here has the advantage that the range of allowed parameter space can be restricted: in this work, we wish to fit the data with two *low-eccentricity* planets. We thus direct the fitting process to model two Keplerian orbits with $e < 0.2$. We note in passing that applying this procedure to the data published in O'Toole et al. (2007) yields a 2-planet system essentially identical

---

[1]Planet data obtained from the Exoplanet Orbit Database at http://exoplanets.org

to that presented in Wittenmyer et al. (2012b). The best-fit set of parameters[2] resulting from 10,000 iterations of the genetic algorithm is then used as initial input for the *Systemic* Console (Meschiari et al. 2009). We then use *Systemic* to perform Keplerian model fits to the data, again requiring $e < 0.2$ for both planets. These results are referred to as Method 2 as given in Table 2.

The 12 systems for which a 2-planet fit gave a physically meaningful result (i.e. no crossing orbits) with χ^2 similar to the one-planet fit were subjected to a more detailed fitting process. We used the Runge-Kutta algorithm within *Systemic* to perform a dynamical fit which accounted for the gravitational interactions between the modelled planets. The model systems were then integrated for 10^5 years as a basic stability check. The results of this analysis, those nine systems which remained stable for 10^5 yr, are given in Table 3. For those systems which proved stable in the initial check, we produced detailed dynamical maps of a broad range of parameter space about the best-fit orbits. For this final step in the dynamical feasibility testing, we turned to the *Mercury* N-body integrator (Chambers 1999). Following our previous work in dynamical mapping of extrasolar planetary systems (Wittenmyer et al. 2012c; Horner et al. 2012b,c; Robertson et al. 2012a,b; Wittenmyer et al. 2012b,a), we sampled a 3σ region of four-dimensional parameter space: semimajor axis (a), eccentricity (e), mean anomaly (M), and argument of periastron (ω). Due to computational limitations and the large uncertainties involved for these speculative 2-planet systems, we chose coarse grids: 21x21x5x5 in (a, e, M, ω), respectively. As in previous work, we held the best-constrained planet (planet 1 as given in Table 3) fixed and altered the initial parameters of the second planet. We ran each simulation for 10^8 yr, or until the system destabilised (via ejection or collision).

3. Results

We give the results of all orbit fits, including the reduced χ^2 and rms velocity scatter, in Table 2. Many of the attempted 2-planet fits resulted in two Keplerians at nearly identical periods. These systems may have a physically plausible solution with a slightly worse χ^2, but testing such possibilities is beyond the scope of this paper. Hence, there may exist additional "good" 2-planet solutions which have been missed by our approach.

---

[2]While genetic algorithms are commonly lauded as ways to find a *global* best fit, we note that their effectiveness depends on the choice of input parameters such as mutation rates and the degree to which χ^2 is allowed to increase between generations. Hence, the "global" solutions found by our approach cannot necessarily be guaranteed to be the absolute best-fit for the the very complicated, multi-modal parameter space of the second planet.

The Keplerian fitting methods used here incorporate no physics: they are simply seeking a lowest-χ^2 solution regardless of the physicality of the resulting system parameters. A 1:1 resonant configuration is dynamically possible, as evidenced by the abundance of such "Trojan" objects in our own Solar system (Levison et al. 1997; Horner & Lykawka 2010; Horner et al. 2012a). However, the radial-velocity signature of a 1:1 configuration is extremely difficult to disentangle (Laughlin & Chambers 2002; Giuppone et al. 2012). Some extrasolar planetary systems have been proposed to host dynamically stable planets in 1:1 configurations (Goździewski & Konacki 2006; Cresswell & Nelson 2009; Schwarz et al. 2009; Funk et al. 2012). However, owing to the difficulty of maintaining dynamically stable configurations, we consider such cases to be beyond the scope of this work. In this section, we will focus on those systems where a 2-planet fit produced a "plausible" result (Table 3) with a χ^2 and rms similar to, or better than, the single-eccentric-planet fit as given in Table 2.

HD 3651 – The best 2-planet fit resulted in a 2:1 period commensurability, with the second signal at $P = 31.08$ days. This is quite close to the monthly observing window, so the fit results in large uncertainties in phase (ω and mean anomaly). The χ^2 and rms are similar to, but slightly higher than, the one-planet fit. Detailed dynamical simulations (Figure 1, panel a) clearly show the 2:1 resonance as a vertical strip of stability throughout the range of allowed eccentricities, and the best fit for a second planet places it comfortably within an extremely stable region.

HD 7449 – The two-planet model results in two giant planets, with minimum masses of 1.2 and 0.4 M_{Jup} (Table 3). The dynamical tests (Figure 1, panel b) show that the best-fit eccentricity for the second (innermost) planet is on the edge of a stable region. As the eccentricity of the second planet is increased beyond $e = 0.4$, the system stability is quickly degraded.

HD 52265 – As with HD 3651, this system also gave a 2:1 configuration, with the second planet at half the period of the known planet, and a slightly worse χ^2 and rms. Figure 1 (panel c) shows that the candidate planet is well within a broad stable region.

HD 65216 – A second planet can be fit, with $P = 152.6\pm0.5$ days and a mass of 0.17 ± 0.03 M_{Jup}. The initial dynamical check in *Systemic* showed this system to be stable, and further dynamical mapping (Figure 1, panel d) shows that the entire 3-sigma $a - e$ parameter space is stable.

HD 85390 – Here, fitting a second planet improves the χ^2 (12.2 to 4.3) and rms ($2.3\,\mathrm{m\,s^{-1}}$ to $1.4\,\mathrm{m\,s^{-1}}$). The eccentricities of both planets are then consistent with zero. The second planet would be a Jupiter analog (e.g. Wittenmyer et al. 2011a), with $P \sim 10$ yr and a mass of $0.20\pm0.02 M_{Jup}$. The detailed dynamical map (Figure 2, panel a) shows a

broad swath of stability for all orbits with $a \gtrsim 2\,\mathrm{AU}$.

HD 89744 – The possible second planet has a period of 85.2 days, very close to a 3:1 commensurability with the known 258-day planet. The dynamics of the system (Figure 2, panel b) show that all permissible orbits are stable, despite the relatively high mass of the candidate planet (3.2 $\mathrm{M_{Jup}}$).

HD 92788 – Figure 2 (panel c) shows this planet candidate is almost certainly trapped in the 2:1 resonance with the known 326-day planet. This resonance would allow relatively large eccentricities (and even crossing orbits) to be long-term stable.

HD 117618 – Adding a second planet improves the χ^2 (8.1 to 5.7) and rms (5.6m s^{-1} to 4.6m s^{-1}). With a period of 318±2 days, the second signal is far enough from one year to allay fears of aliasing. A dynamical map for this Saturn-mass candidate is shown in Figure 2 (panel d) – again, there is a vast region of stability across the 3σ parameter space.

GJ 649 – As the two proposed planets are very widely separated, and of low mass, we did not perform the dynamical testing for this system. The planet candidates are separated by 21.8 mutual Hill radii, which is certainly sufficient dynamical room for any interaction to be negligible (Chambers et al. 1996).

HD 192310 (=GJ 785) – While this system does not appear in Table 3, we note that the 2-planet fit shown in Table 2 suggests a Neptune-mass second planet with period 629±64 days. This is broadly consistent (within $\sim 1.5\sigma$) with the claim of a 0.07$\mathrm{M_{Jup}}$ planet by Pepe et al. (2011), with $P = 526\pm9$ days.

Anglada-Escudé et al. (2010) have also approached this problem of disentangling single eccentric planets from near-circular two-planet systems, specifically considering the case of the 2:1 resonance. That work showed that about 35% of known single-planet systems were indistiguishable from 2:1 resonant solutions. By comparison, 9/82=11% of the systems examined in the present work resulted in a 2:1 configuration (Table 2). We also find that a further 24/82=29% of systems tested resulted in co-orbital (1:1) configurations. Hollis et al. (2012) also performed an extensive and self-consistent Bayesian re-analysis of available radial-velocity data for 94 exoplanet systems. As part of their analysis, they attempted two-planet fits to the known single-planet systems (Hollis et al. 2012, Table A2). Unlike this work, their two-planet fits were not restricted to low eccentricities. For example, Hollis et al. (2012) find a two-planet solution for HD 3651 where $(P_1, e_1) = (62.25, 0.60)$ and $(P_2, e_2) = (295, 0.32)$. By contrast, our result in Table 3 gives a 2:1 configuration with $e \lesssim 0.06$ for both planets.

Ultimately, there is no substitute for sampling density: given infinite observational resources, one would ideally observe every system as often as possible (O'Toole et al. 2009c).

Such techniques have been successful in identifying low-mass planets (O'Toole et al. 2009b; Vogt et al. 2010; Dumusque et al. 2012) and in clarifying the true orbital period and mass of eccentric planets where large velocity excursions occur on short timescales (Cochran et al. 2004; Endl et al. 2006). It is, of course, more practical to optimally plan one's observations to confirm suspected planet candidates (Ford 2008). All of the systems discussed above withstood detailed dynamical scrutiny, as shown in Figures 1 and 2. For those potential 2-planet systems, we now ask how one may observationally discern between the one- and two-planet models. At present, the two models are typically close to each other in goodness-of-fit; an example is shown in Figure 3 for HD 65216. In the future, however, the two possible models may diverge. In Figures 4–8, we overplot the two models for each system, to give a qualitative estimate of the optimal times to observe them. When they diverge sufficiently, well-timed observations of reasonable precision ($\sim$2-3 m s^{-1}) can distinguish between the 1- and 2-planet models. We note, however, that the 2-planet fits often have large phase gaps (and hence relatively large uncertainties in P and T_0) which can shift the model curves shown here. For this reason, we leave more detailed quantitative simulations of detectability (e.g. Wittenmyer et al. 2013) for future work.

4. Summary and Conclusions

We have examined 82 known moderately eccentric single-planet systems, reanalysing the available radial-velocity data to test the hypothesis that some may actually be low-eccentricity two-planet systems. We have identified nine particularly promising candidate systems, and performed detailed dynamical stability simulations of the candidate planets. All of the systems proved to be dynamically stable on timescales of at least 10^8 yr. We have also given model orbits to show qualitatively when the one- and two-planet solutions diverge enough to be distinguishable by future well-timed radial-velocity observations. Our results suggest that at least 11% of apparently single-planet systems may in fact host two low-eccentricity planets, a figure likely to rise as more observations are obtained. The difference between the one- and two-planet solutions should typically be observable within the next 3 years, adding weight to the case for continued observations of these systems.

REFERENCES

Anglada-Escudé, G., López-Morales, M., & Chambers, J. E. 2010, ApJ, 709, 168

Arriagada, P., Butler, R. P., Minniti, D., et al. 2010, ApJ, 711, 1229

Butler, R. P., et al. 2006, ApJ, 646, 505

Chambers, J. E. 1999, MNRAS, 304, 793

Chambers, J. E., Wetherill, G. W., & Boss, A. P. 1996, Icarus, 119, 261

Cochran, W. D., Endl, M., Wittenmyer, R. A., & Bean, J. L. 2007, ApJ, 665, 1407

Cochran, W. D., Endl, M., McArthur, B., et al. 2004, ApJ, 611, L133

Correia, A. C. M., Udry, S., Mayor, M., et al. 2008, A&A, 479, 271

Cumming, A., Butler, R. P., Marcy, G. W., Vogt, S. S., Wright, J. T., & Fischer, D. A. 2008, PASP, 120, 531

Cresswell, P., & Nelson, R. P. 2009, A&A, 493, 1141

da Silva, R., Udry, S., Bouchy, F., et al. 2006, A&A, 446, 717

da Silva, R., Udry, S., Bouchy, F., et al. 2007, A&A, 473, 323

Díaz, R. F., Santerne, A., Sahlmann, J., et al. 2012, A&A, 538, A113

Döllinger, M. P., Hatzes, A. P., Pasquini, L., et al. 2009, A&A, 499, 935

Dumusque, X., Pepe, F., Lovis, C., et al. 2012, Nature, 491, 207

Dumusque, X., Lovis, C., Ségransan, D., et al. 2011, A&A, 535, A55

Eggenberger, A., Mayor, M., Naef, D., et al. 2006, A&A, 447, 1159

Endl, M., Hatzes, A. P., Cochran, W. D., et al. 2004, ApJ, 611, 1121

Endl, M., Cochran, W. D., Wittenmyer, R. A., & Hatzes, A. P. 2006, AJ, 131, 3131

Fischer, D., Driscoll, P., Isaacson, H., et al. 2009, ApJ, 703, 1545

Fischer, D. A., Vogt, S. S., Marcy, G. W., et al. 2007, ApJ, 669, 1336

Ford, E. B. 2008, AJ, 135, 1008

Ford, E. B., & Rasio, F. A. 2008, ApJ, 686, 621

Forveille, T., Bonfils, X., Lo Curto, G., et al. 2011, A&A, 526, A141

Frink, S., Mitchell, D. S., Quirrenbach, A., et al. 2002, ApJ, 576, 478

Funk, B., Schwarz, R., Süli, Á., & Érdi, B. 2012, MNRAS, 423, 3074

Gettel, S., Wolszczan, A., Niedzielski, A., et al. 2012, ApJ, 745, 28

Giuppone, C. A., Benítez-Llambay, P., & Beaugé, C. 2012, MNRAS, 421, 356

Goździewski, K., & Konacki, M. 2006, ApJ, 647, 573

Haghighipour, N., Vogt, S. S., Butler, R. P., et al. 2010, ApJ, 715, 271

Hollis, M. D. J., Balan, S. T., Lever, G., & Lahav, O. 2012, MNRAS, 423, 2800

Horner, J., & Lykawka, P. S. 2010, MNRAS, 405, 49

Horner, J., Lykawka, P. S., Bannister, M. T., & Francis, P. 2012a, MNRAS, 422, 2145

Horner, J., Wittenmyer, R. A., Hinse, T. C., & Tinney, C. G. 2012b, MNRAS, 425, 749

Horner, J., Hinse, T. C., Wittenmyer, R. A., Marshall, J. P., & Tinney, C. G. 2012c, MNRAS, 427, 2812

Howard, A. W., Johnson, J. A., Marcy, G. W., et al. 2010a, ApJ, 721, 1467

Howard, A. W., et al. 2010b, Science, 330, 653

Howard, A. W., Johnson, J. A., Marcy, G. W., et al. 2011, ApJ, 730, 10

Jenkins, J. S., Jones, H. R. A., Goździewski, K., et al. 2009, MNRAS, 398, 911

Johnson, J. A., Marcy, G. W., Fischer, D. A., et al. 2006, ApJ, 647, 600

Johnson, J. A., Fischer, D. A., Marcy, G. W., et al. 2007, ApJ, 665, 785

Johnson, J. A., Howard, A. W., Marcy, G. W., et al. 2010, PASP, 122, 149

Johnson, J. A., Clanton, C., Howard, A. W., et al. 2011, ApJS, 197, 26

Jones, H. R. A., Paul Butler, R., Marcy, G. W., et al. 2002, MNRAS, 337, 1170

Jones, H. R. A., Butler, R. P., Tinney, C. G., et al. 2006, MNRAS, 369, 249

Laughlin, G., & Chambers, J. E. 2002, AJ, 124, 592

Levison, H. F., Shoemaker, E. M., & Shoemaker, C. S. 1997, Nature, 385, 42

Lo Curto, G., Mayor, M., Benz, W., et al. 2010, A&A, 512, A48

López-Morales, M., Butler, R. P., Fischer, D. A., et al. 2008, AJ, 136, 1901

Marcy, G. W., Butler, R. P., Vogt, S. S., et al. 2005, ApJ, 619, 570

Mayor, M., Udry, S., Naef, D., et al. 2004, A&A, 415, 391

Meschiari, S., Wolf, A. S., Rivera, E., et al. 2009, PASP, 121, 1016

Meschiari, S., Laughlin, G., Vogt, S. S., et al. 2011, ApJ, 727, 117

Mordasini, C., Mayor, M., Udry, S., et al. 2011, A&A, 526, A111

Moutou, C., Mayor, M., Lo Curto, G., et al. 2009, A&A, 496, 513

Moutou, C., Mayor, M., Lo Curto, G., et al. 2011, A&A, 527, A63

Naef, D., Mayor, M., Pepe, F., et al. 2001, A&A, 375, 205

Naef, D., et al. 2001, A&A, 375, L27

Naef, D., Mayor, M., Beuzit, J. L., et al. 2004, A&A, 414, 351

Naef, D., Mayor, M., Benz, W., et al. 2007, A&A, 470, 721

O'Toole, S. J., Butler, R. P., Tinney, C. G., et al. 2007, ApJ, 660, 1636

O'Toole, S. J., Tinney, C. G., Jones, H. R. A., et al. 2009a, MNRAS, 392, 641

O'Toole, S., Tinney, C. G., Butler, R. P., et al. 2009b, ApJ, 697, 1263

O'Toole, S. J., Jones, H. R. A., Tinney, C. G., et al. 2009c, ApJ, 701, 1732

Peek, K. M. G., Johnson, J. A., Fischer, D. A., et al. 2009, PASP, 121, 613

Pepe, F., Lovis, C., Ségransan, D., et al. 2011, A&A, 534, A58

Pepe, F., Mayor, M., Galland, F., et al. 2002, A&A, 388, 632

Perrier, C., Sivan, J.-P., Naef, D., Beuzit, J. L., Mayor, M., Queloz, D., & Udry, S. 2003, A&A, 410, 1039

Robertson, P., Horner, J., Wittenmyer, R. A., et al. 2012b, ApJ, 754, 50

Robertson, P., Endl, M., Cochran, W. D., et al. 2012a, ApJ, 749, 3

Rodigas, T. J., & Hinz, P. M. 2009, ApJ, 702, 716

Santos, N. C., Mayor, M., Naef, D., et al. 2001, A&A, 379, 999

Santos, N. C., Udry, S., Bouchy, F., et al. 2008, A&A, 487, 369

Santos, N. C., Mayor, M., Benz, W., et al. 2010, A&A, 512, A47

Santos, N. C., Mayor, M., Bonfils, X., et al. 2011, A&A, 526, A112

Schwarz, R., Süli, Á., Dvorak, R., & Pilat-Lohinger, E. 2009, Celestial Mechanics and Dynamical Astronomy, 104, 69

Ségransan, D., Udry, S., Mayor, M., et al. 2010, A&A, 511, A45

Shen, Y., & Turner, E. L. 2008, ApJ, 685, 553

Sozzetti, A., Udry, S., Zucker, S., et al. 2006, A&A, 449, 417

Tamuz, O., Ségransan, D., Udry, S., et al. 2008, A&A, 480, L33

Tinney, C. G., Butler, R. P., Marcy, G. W., et al. 2003, ApJ, 587, 423

Tinney, C. G., Butler, R. P., Marcy, G. W., et al. 2005, ApJ, 623, 1171

Tinney, C. G., Butler, R. P., Jones, H. R. A., et al. 2011a, ApJ, 727, 103

Tinney, C. G., Wittenmyer, R. A., Butler, R. P., Jones, H. R. A., O'Toole, S. J., Bailey, J. A., Carter, B. D., & Horner, J. 2011b, ApJ, 732, 31

Udry, S., Mayor, M., Naef, D., et al. 2002, A&A, 390, 267

Vogt, S. S., Butler, R. P., Marcy, G. W., et al. 2002, ApJ, 568, 352

Vogt, S. S., et al. 2010, ApJ, 708, 1366

Wittenmyer, R. A., Endl, M., Cochran, W. D., & Levison, H. F. 2007, AJ, 134, 1276

Wittenmyer, R. A., Endl, M., Cochran, W. D., Levison, H. F., & Henry, G. W. 2009, ApJS, 182, 97

Wittenmyer, R. A., O'Toole, S. J., Jones, H. R. A., Tinney, C. G., Butler, R. P., Carter, B. D., & Bailey, J. 2010, ApJ, 722, 1854

Wittenmyer, R. A., Tinney, C. G., O'Toole, S. J., Jones, H. R. A., Butler, R. P., Carter, B. D., & Bailey, J. 2011a, ApJ, 727, 102

Wittenmyer, R. A., Tinney, C. G., Butler, R. P., et al. 2011b, ApJ, 738, 81

Wittenmyer, R. A., Endl, M., Wang, L., et al. 2011c, ApJ, 743, 184

Wittenmyer, R. A., Horner, J., Marshall, J. P., Butters, O. W., & Tinney, C. G. 2012a, MNRAS, 419, 3258

Wittenmyer, R. A., Horner, J., Tuomi, M., et al. 2012b, ApJ, 753, 169

Wittenmyer, R. A., Horner, J., & Tinney, C. G. 2012c, ApJ, 761, 165

Wittenmyer, R. A., Tinney, C. G., Horner, J., et al. 2013, PASP, 125, 351

Wright, J. T., Upadhyay, S., Marcy, G. W., et al. 2009, ApJ, 693, 1084

Wright, J. T., et al. 2011, PASP, 123, 412

Zhou, J.-L., Lin, D. N. C., & Sun, Y.-S. 2007, ApJ, 666, 423

Table 1.   Summary of Radial-Velocity Data

Star	N	Source
HD 1237	61	Naef et al. (2001)
HD 1690	41	Moutou et al. (2011)
HD 2039	46	Tinney et al. (2003)[a]
HD 3651	163	Butler et al. (2006)
HD 3651	35	Wittenmyer et al. (2009)
HD 4113	130	Tamuz et al. (2008)
HD 4203	23	Butler et al. (2006)
HD 5388	68	Santos et al. (2010)
HD 7449	82	Dumusque et al. (2011)
HD 8574	41	Perrier et al. (2003)
HD 8574	60	Wittenmyer et al. (2009)
HD 8574	26	Butler et al. (2006)
HD 11506	26	Fischer et al. (2007)
HD 16175	44	Peek et al. (2009)
HD 20782	47	Jones et al. (2006)[a]
HD 20868	48	Moutou et al. (2009)
HD 22781	32	Díaz et al. (2012)
HD 23127	44	O'Toole et al. (2007)[a]
HD 30562	45	Fischer et al. (2009)
HD 31253	39	Meschiari et al. (2011)
HD 33283	25	Johnson et al. (2006)
HD 33636	32	Vogt et al. (2002)
HD 38283	61	Tinney et al. (2011b)[a]
HD 39091	67	Jones et al. (2002)[a]
HD 45350	73	Endl et al. (2006)
HD 45350	30	Marcy et al. (2005)
HD 45652	45	Santos et al. (2008)
HD 52265	91	Naef et al. (2001)
HD 52265	28	Butler et al. (2006)
HD 65216	70	Mayor et al. (2004)
HD 81040	26	Sozzetti et al. (2006)
HD 85390	58	Mordasini et al. (2011)
HD 86264	37	Fischer et al. (2009)
HD 87883	69	Fischer et al. (2009)
HD 89744	50	Butler et al. (2006)
HD 89744	42	Wittenmyer et al. (2009)
HD 90156	66	Mordasini et al. (2011)
HD 92788	55	Mayor et al. (2004)
HD 92788	58	Butler et al. (2006)
HD 96127	50	Gettel et al. (2012)
HD 96167	47	Peek et al. (2009)
HD 99706	24	Johnson et al. (2011)
HD 100777	29	Naef et al. (2007)
HD 102365	168	Tinney et al. (2011a)[a]
HD 106252	40	Perrier et al. (2003)
HD 106252	70	Wittenmyer et al. (2009)

Table 1—Continued

Star	N	Source
HD 106270	20	Johnson et al. (2011)
HD 108147	57	AAT[a]
HD 108147	118	Pepe et al. (2002)
HD 117618	70	Tinney et al. (2005)[a]
HD 118203	43	da Silva et al. (2006)
HD 126614A	70	Howard et al. (2010a)
HD 131664	41	Moutou et al. (2009)
HD 132406	21	da Silva et al. (2007)
HD 136118	37	Butler et al. (2006)
HD 136118	68	Wittenmyer et al. (2009)
HD 137388	62	Dumusque et al. (2011)
HD 137510	76	Endl et al. (2004)
HD 137510	13	Díaz et al. (2012)
HD 141937	81	Udry et al. (2002)
HD 142022	76	Eggenberger et al. (2006)
HD 142415	137	Mayor et al. (2004)
HD 142415	22	AAT[a]
HD 145377	64	Moutou et al. (2009)
HD 153950	49	Moutou et al. (2009)
HD 154672	6	Jenkins et al. (2009)
HD 154672	16	López-Morales et al. (2008)
HD 156279	15	Díaz et al. (2012)
HD 156846	54	Tamuz et al. (2008)
HD 171028	19	Santos et al. (2011)
HD 171238	99	Ségransan et al. (2010)
HD 175541	29	Johnson et al. (2007)
HD 175167	13	Arriagada et al. (2010)
HD 187085	64	Jones et al. (2006)[a]
HD 190228	51	Perrier et al. (2003)
HD 190228	50	Wittenmyer et al. (2009)
HD 196885	76	Fischer et al. (2009)
HD 196885	102	Correia et al. (2008)
HD 204941	35	Dumusque et al. (2011)
HD 210277	69	Butler et al. (2006)
HD 210277	21	Wittenmyer et al. (2007)
HD 210277	42	Naef et al. (2001)
HD 213240	72	Santos et al. (2001)
HD 213240	35	AAT[a]
HD 217786	17	Moutou et al. (2011)
HD 216437	50	Jones et al. (2002)[a]
HD 216437	21	Mayor et al. (2004)
HD 216770	16	Mayor et al. (2004)
HD 218566	56	Meschiari et al. (2011)
HD 222582	37	Butler et al. (2006)
HD 240237	40	Gettel et al. (2012)
HIP 2247	26	Moutou et al. (2009)

Table 1—Continued

Star	N	Source
HIP 5158	54	Lo Curto et al. (2010)
iota Dra	119	Butler et al. (2006)
iota Dra	56	Frink et al. (2002)
GJ 649	43	Johnson et al. (2010)
GJ 785	75	Howard et al. (2011)
HIP 57050	37	Haghighipour et al. (2010)
GJ 676A	69	Forveille et al. (2011)
14 Her	49	Butler et al. (2006)
14 Her	35	Wittenmyer et al. (2007)
14 Her	119	Naef et al. (2004)
42 Dra	45	Döllinger et al. (2009)
70 Vir	74	Butler et al. (2006)
70 Vir	35	Naef et al. (2004)

[a]Includes additional unpublished AAPS data, given in Tables A1-A12 in the Appendix.

Table 2.   Summary of Results

Star	Method	χ^2_ν	RMS (m s^{-1})	P_1 (days)	$m_1 \sin i$ (M$_{\rm Jup}$)	M_1 (degrees)	e_1	ω_1 degrees	P_2 (days)	$m_2 \sin i$ (M$_{\rm Jup}$)	M_2 (degrees)	e_2	ω_2 (degrees)
HD 1237	1[a]	3.40	18.9	133.7(2)	3.4(2)	317(2)	0.51(2)	291(3)					
	2[b]	10.06	31.1	117.6(6.6)	4(12)	140(32)	0.18(10)	16(48)	106.9(10.2)	4(11)	71(26)	0.2(0.2)	192(52)
HD 1690	1	359.7	35.3	527(2)	4.7(5)	77(5)	0.74(11)	103(13)					
	2	353.5	30.35	494(11)	8(8)	265(33)	0.06(23)	243(44)	401.3(8.8)	5(4)	302(42)	0.2(0.2)	328(37)
HD 2039	1	6.43	13.7	1110(3)	4.5(1.1)	57(7)	0.64(6)	342(3)					
	2	35.83	27.3	1075(49)	6(7)	338(57)	0.02(31)	304(38)	1095(19)	7(7)	13(55)	0.19(16)	70(35)
HD 3651	1	3.82	6.3	62.22(1)	0.23(1)	121(9)	0.60(4)	243(5)					
	2	5.68	6.8	62.20(0.04)	0.22(3)	241(33)	0.03(33)	112(21)	31.07(2)	0.09(5)	78(65)	0.0(2)	328(35)
HD 4113	1	4.28	9.5	526.61(8)	1.66(7)	217.1(3)	0.899(6)	320(2)					
	2	215.83	71.0	506(14)	3.1(1.6)	15(16)	0.00(38)	111(34)	404.6(2.2)	2.7(2.1)	314(46)	0.18(23)	268(20)
HD 4203	1	4.14	5.8	434(2)	2.2(7)	226(14)	0.7(1)	346(5)					
	2	35.66	12.9	422.6(11.3)	2.6(2.0)	156(53)	0.15(21)	94(70)	433(22)	2.6(2.0)	259(41)	0.20(35)	219(65)
HD 5388	1	2.64	4.1	777.2(3.5)	2.0(1)	284(6)	0.40(2)	324(4)					
	2	4.07	4.8	776(39)	2.4(1.7)	255(21)	0.16(20)	52(30)	769.3(30.1)	2.2(1.6)	317(18)	0.18(20)	208(23)
HD 7449	1	47.58	4.2	1251(17)	1.6(7)	56(5)	0.848	337(3)					
	2	71.15	5.8	1494(138)	3.2(3.0)	82(32)	0.2(9)	5(57)	1738(1465)	2.8(3.4)	65(46)	0.1(3)	254(40)
HD 8574	1	2.21	14.0	227.0(2)	1.81(8)	36(6)	0.30(3)	27(5)					
	2	2.33	15.0	227.4(2)	1.98(7)	56(46)	0.12(4)	11(66)	17.75(2)	0.13(10)	105(35)	0.1(3)	190(30)
HD 11506	1	15.88	9.79	1436(102)	5.0(7)	194(17)	0.43(17)	270(9)					
	2	9.9	6.6	1333(683)	4.7(1.1)	220(22)	0.1(2)	245(51)	370	1(6)	41(33)	0.2(2)	221(50)
HD 16175	1	2.36	8.6	990(9)	4.4(3)	189(4)	0.60(3)	221(3)					
	2	5.83	13.7	1087(32)	9(2)	302(14)	0.02(5)	279	1026(19)	12(2)	234(18)	0.2	163
HD 20782	1	6.56	6.5	597.08(6)	1.35(9)	340.5(2)	0.960	140(2)					
	2	385.25	36.2	586(27)	5(2)	356(30)	0.1(1)	16(36)	595(82)	4.6(3.1)	281(25)	0.19(8)	279(57)
HD 20868	1	1.63	1.8	380.85(9)	1.99(9)	15.7(3)	0.755(2)	356.2(4)					
	2	250.83	21.4	409.8(9.4)	3.0(1.3)	135(35)	0.17(21)	307(31)	50.4(2.3)	1.0(1.2)	286(56)	0.12(28)	103(29)
HD 22781	1	9.54	13.0	528.1(2)	13.9(7)	173.3(2)	0.819(3)	316.5(8)					
	2	1002.75	121.1	500(18)	23(18)	147(39)	0.1(3)	291(40)	105(4)	7(7)	65(41)	0.2(2)	33(46)
HD 23127	1	8.36	11.7	1237(14)	1.5(1)	324(16)	0.37(7)	197(13)					
	2	19.55	13.5	1233.6(17.3)	1.8(0.3)	313(57)	0.15(10)	208(78)	9.91(13)	0.08(17)	216(50)	0.04(30)	149(41)
HD 30562	1	2.49	7.1	1159(16)	1.35(6)	326(21)	0.76(3)	79(6)					
	2	8.17	12.8	1131.4(24.4)	2.5(1.4)	314(59)	0.16(10)	95(28)	825(756)	2.0(1.6)	290(24)	0.20(9)	321(48)
HD 31253	1	8.87	4.3	465.4(1.8)	0.50(5)	138(16)	0.34(10)	244(16)					

Table 2—Continued

Star	Method	χ^2_ν	RMS (m s^{-1})	P_1 (days)	$m_1 \sin i$ (M$_{\rm Jup}$)	M_1 (degrees)	e_1	ω_1 degrees	P_2 (days)	$m_2 \sin i$ (M$_{\rm Jup}$)	M_2 (degrees)	e_2	ω_2 (degrees)
	2	6.47	3.4	463.4(3.2)	0.51(8)	134(55)	0.08(11)	248(42)	686.0(15.9)	0.3(5)	4(43)	0.05(29)	128(47)
HD 33283	1	0.64	3.2	18.179(6)	0.33(2)	305(4)	0.48(4)	156(7)					
	2	0.56	2.6	18.12(4)	0.37(9)	243(27)	0.1(1)	230(65)	47.6(3)	0.4(2)	32(10)	0.2(2)	11(73)
HD 33636	1	2.13	8.7	1552(135)	7.8(5)	276(8)	0.39(3)	335(5)					
	2	19.01	16.0	2204(613)	9.5(3.9)	153(63)	0.09(16)	121(31)	970(136)	4.3(3.1)	195(58)	0.20(19)	18(48)
HD 38283	1	7.90	5.6	360.4(9)	0.5(2)	150(11)	0.64(26)	57(21)					
	2	6.73	4.8	354.5(3.7)	0.6(2.6)	66(43)	0.16(14)	127(51)	364.5(4.2)	0.4(2.5)	357(42)	0.17(24)	320(59)
HD 39091	1	11.3	6.2	2088(3)	9.7(3)	137(1)	0.643(5)	331.5(7)					
	2	685.05	43.8	2093(33)	7.5(8)	356(8)	0.002	110	1056(11)	5.0(5)	295(18)	0.2	314
HD 45350	1	1.50	8.0	964(3)	1.8(1)	14(3)	0.778(9)	343(2)					
	2	12.86	16.9	989(23)	3.4(7.8)	225(27)	0.17(6)	99(43)	953(40)	3.7(7.8)	272(24)	0.17(13)	232(34)
HD 45652	1	2.88	13.6	43.7(1)	0.47(4)	87(13)	0.45(6)	249(11)					
	2	3.71	12.6	43.83(24)	0.6(1)	66(43)	0.17(11)	281(16)	95.6(4.2)	0.3(3)	9(45)	0.17(22)	7(38)
HD 52265	1	2.02	10.9	119.31(78)	1.12(6)	24(5)	0.35(3)	232(6)					
	2	2.31	10.8	119.38(25)	1.31(7)	19(64)	0.19(5)	243(39)	179.1(4.0)	0.33(24)	317(55)	0.06(22)	168(53)
HD 65216	1	1.73	7.1	612(10)	1.22(7)	289(17)	0.41(6)	198(7)					
	2	1.57	6.5	574.2(7.1)	1.4(2)	3(66)	0.15(8)	82(34)	270.7(3.3)	0.4(2)	294(59)	0.02(9)	298(22)
HD 81040	1	5.68	27.9	1005(10)	6.7(4)	286(37)	0.59(4)	85(4)					
	2	4.02	22.8	1091(23)	9(4)	15(69)	0.18(17)	51(27)	262.2(6.9)	2(3)	250(24)	0.20(29)	19(49)
HD 85390	1	12.22	2.3	806(19)	0.11(1)	62(39)	0.59(fixed)	301(10)					
	2	5.56	1.6	799(34)	0.14(1)	22(21)	0.01(13)	307(18)	2491(5399)	0.18(15)	305(39)	0.03(26)	151(42)
HD 86264	1	2.76	26.9	1520(34)	6.8(4)	284(37)	0.82(17)	296(27)					
	2	3.2	30.9	1416(66)	9(4)	276(29)	0.1(2)	310(22)	194(12)	2(2)	119(51)	0.16(30)	318(42)
HD 87883	1	4.16	8.9	2762(11)	1.8(2)	2(7)	0.55(17)	290(16)					
	2	3.88	8.6	2934(113)	2.1(3)	44(6)	0.17	283	342(2)	0.3(1)	95(15)	0.20	305
HD 89744	1	2.58	15.2	256.78(5)	8.5(3)	321.5(5)	0.673(7)	195(1)					
	2	58.5	72.3	256.7(1)	11.9(1.3)	325(51)	0.20(2)	189(48)	256(344)	5(2)	201(53)	0.2(3)	118(53)
HD 90156	1	9.99	1.2	49.79(6)	0.055(5)	218(13)	0.34(6)	112(12)					
	2	8.56	1.1	49.65(7)	0.069(5)	207(60)	0.18(10)	98(37)	13.52(4)	0.015(14)	292(37)	0.03(29)	19(62)
HD 92788	1	2.29	8.6	325.7(2)	3.5(1)	80(3)	0.336(9)	276(2)					
	2	4.04	10.3	325(3)	4(1)	44(53)	0.16(15)	0(58)	327(6)	3(2)	132(47)	0.2(2)	152(45)
HD 96127	1	77.56	49.2	636(19)	4.1(9)	191(39)	0.36(13)	155(7)					
	2	39.53	40.0	652(16)	3.7(5)	227(47)	0.18	128	5.573(2)	0.50(9)	227(25)	0.10	228

Table 2—Continued

Star	Method	χ^2_ν	RMS (m s^{-1})	P_1 (days)	$m_1 \sin i$ (M$_{\rm Jup}$)	M_1 (degrees)	e_1	ω_1 degrees	P_2 (days)	$m_2 \sin i$ (M$_{\rm Jup}$)	M_2 (degrees)	e_2	ω_2 (degrees)
HD 96167	1	11.32	4.4	498(2)	0.68(4)	329(6)	0.71(6)	288(9)					
	2	20.96	6.4	518	1(1)	283(54)	0.0(0.4)	153(51)	508(8)	1.4(1.0)	339(52)	0.2(2)	268(28)
HD 99706	1	23.57	5.7	812(22)	1.7(1)	16(17)	0.31(9)	357(17)					
	2	16.8	3.9	853(71)	1.8(9)	246(25)	0.2(2)	159(62)	379(19)	0.6(1.0)	111(46)	0.1(3)	249(32)
HD 100777	1	1.49	1.8	383.7(1.1)	1.16(6)	352(2)	0.358(18)	203(3)					
	2	1.86	1.7	382.8(3.6)	1.3(7)	33(46)	0.16(14)	155(50)	127.3(2.9)	0.18(16)	308(34)	0.12(26)	199(39)
HD 102365	1	10.70	3.8	122.1(4)	0.048(8)	322(31)	0.17(16)	56(fixed)					
	2	9.31	3.5	122.18(73)	0.07(3)	276(61)	0.07(21)	105(51)	927(35)	0.1(2)	233(56)	0.00(36)	44(53)
HD 106252	1	1.42	12.2	1531(5)	7.0(3)	41(2)	0.48(1)	293(2)					
	2	3.34	17.5	1510(12)	6.8(2)	26(38)	0.07(3)	303(22)	760	2(2)	44(32)	0.2(2)	348(41)
HD 106270	1	30.1	8.5	2658(880)	11(2)	277(27)	0.36(15)	16(6)					
	2	49.38	8.5	2539(271)	12(4)	302(28)	0.14(15)	345(55)	885(82)	1.3(2.3)	83(51)	0.2(3)	26(42)
HD 108147	1	6.06	15.4	10.9013(7)	0.31(2)	60(4)	0.53(4)	307(5)					
	2	7.58	16.4	10.902(1)	0.34(2)	71(31)	0.17(6)	300(38)	91.1(9)	0.2(2)	118(30)	0.04(32)	36(28)
HD 117618	1	8.11	5.6	25.815(6)	0.20(2)	334(18)	0.33(9)	256(15)					
	2	5.88	4.7	25.81(1)	0.21(2)	323(64)	0.08(10)	256(46)	319.1(4.2)	0.2(2)	283(60)	0.00(32)	32(25)
HD 118203	1	2.26	19.6	6.1345(9)	2.13(9)	149(4)	0.31(2)	155.7(3.6)					
	2	6.72	31.2	6.135(2)	2.31(6)	152(59)	0.145(35)	154(63)	29.0(1.0)	0.5(4)	168(29)	0.18(25)	336(54)
HD 126614	1	8.87	3.8	1245(12)	0.39(3)	328(11)	0.43(9)	241(14)					
	2	11.03	4.3	1212(24)	0.4(2)	218(33)	0.04(20)	340(28)	339(18)	0.1(2)	192(30)	0.0(3)	288(43)
HD 131664	1	6.06	5.7	1951(42)	18(1)	200(9)	0.64(2)	150(1)					
	2	347.83	27.7	1825(17)	24(3)	176(87)	0.16(8)	189(77)	1584(116)	15(4)	243(49)	0.20(13)	307(48)
HD 132406	1	1.74	13.2	975(50)	5.6(1.6)	241(22)	0.34(12)	214(24)					
	2	2.00	11.1	950(124)	5.5(2.6)	264(35)	0.04(18)	192(54)	29.2(2)	0.5(5)	171(42)	0.07(34)	120(48)
HD 136118	1	1.82	16.5	1187.3(2.4)	11.7(4)	61(3)	0.338(15)	320(2)					
	2	2.76	20.0	1190.1(21.2)	13(4)	66(13)	0.198(40)	310(45)	1291.6(9999)	2(4)	51(37)	0.04(36)	157(38)
HD 137388	1	17.05	3.2	355.6(2.6)	0.32(4)	318(33)	0.13(9)	269(31)					
	2	13.16	2.5	330.7(4.4)	0.3(2)	43(51)	0.17(15)	60.1(9.6)	2436(2134)	0.5(6)	329(57)	0.16(13)	139(41)
HD 137510	1	5.24	20.4	800.9(5)	26.4(1.2)	37(1)	0.399(8)	32(1)					
	2	17.64	38.1	802(4)	30(14)	47(53)	0.19(5)	11(68)	804(54)	10(14)	315(34)	0.2(9)	245(39)
HD 141937	1	2.69	9.6	653(2)	9.4(6)	41(2)	0.41(2)	187.7(1.3)					
	2	4.33	11.6	659.5(8.7)	11(1)	54(45)	0.183(23)	166(7)	668(34)	3.9(5)	300(30)	0.17(24)	74(74)
HD 142022	1	1.54	10.4	1931(35)	4.3(1.0)	79(9)	0.52(8)	169(5)					

Table 2—Continued

Star	Method	χ^2_ν	RMS (m s^{-1})	P_1 (days)	$m_1 \sin i$ (M$_{\rm Jup}$)	M_1 (degrees)	e_1	ω_1 degrees	P_2 (days)	$m_2 \sin i$ (M$_{\rm Jup}$)	M_2 (degrees)	e_2	ω_2 (degrees)
	2	2.05	10.7	1894(41)	3(2)	260(24)	0.01(28)	342(47)	946(31)	1(2)	32(23)	0.17(17)	296(40)
HD 142415	1	15.03	14.8	406.6(9)	1.8(1)	104(3)	0.64(2)	222(4)					
	2	19.82	17.0	407.7(4.3)	2.2(2.7)	182(63)	0.19(13)	258(37)	397(48)	1.2(3.0)	263(42)	0.16(26)	328(47)
HD 145377	1	104.0	16.8	103.96(17)	5.8(2)	176(5)	0.307(17)	138(3)					
	2	92.50	17.2	103.31(15)	5.7(1)	147(69)	0.074(35)	150(50)	51.1(3.3)	0.9(6)	319(44)	0.09(32)	74(156)
HD 153950	1	5.77	4.5	499.4(3.6)	2.7(1)	251(9)	0.34(2)	308(2)					
	2	8.84	6.2	478.6(8.9)	3.1(2)	218(32)	0.16(6)	303(31)	205(67)	0.4(3)	206(56)	0.10(31)	188(29)
HD 154672	1	3.83	4.4	163.4(1)	5.0(2)	124(2)	0.629(8)	265(1)					
	2	167.55	29.7	165.06(87)	5.7(5)	329(60)	0.07(12)	270(35)	20.4(5)	1.9(1.5)	66(58)	0.09(29)	94(53)
HD 156279	1	8.18	9.7	131.1(5)	9.7(4)	184(2)	0.71(2)	264(2)					
	2	1284.06	74.7	144(9)	14(8)	246(50)	0.1(2)	209(41)	151(8855)	11(7)	148(54)	0.2(3)	102(50)
HD 156846	1	5.18	25.8	359.3(1)	10.9(3)	205.3(4)	0.846(2)	52.3(5)					
	2	1615.61	163.2	344.8(16.4)	18(8)	279(50)	0.00(29)	322(27)	175.7(1.7)	11(3)	36(60)	0.12(5)	332(51)
HD 171028	1	5.29	2.5	550(3)	1.95(8)	146(3)	0.593(8)	304(1)					
	2	578.90	35.0	546.97	2.1(3)	288(1)	0.03	235	546.90	2.1(3)	288(1)	0.03	55
HD 171238	1	7.20	12.9	1466(33)	2.8(2)	250(22)	0.26(4)	75.7(9.7)					
	2	6.81	12.9	1517(105)	3.2(2)	288(36)	0.20(6)	53(30)	122.7(2.7)	0.2(3)	332(6)	0.04(28)	115(28)
HD 175167	1	2.70	5.3	1290(12)	7.8(1.5)	246(11)	0.54(7)	343(7)					
	2	6.95	7.9	1386(23)	7.9(6)	31(7)	0.10	204	302(3)	2.0(3)	0(14)	0.16	126
HD 175541	1	7.15	5.1	297.3(1.3)	0.58(6)	90(20)	0.31(10)	179(19)					
	2	6.72	4.3	295.0(1.7)	0.6(1)	79(38)	0.09(14)	181(59)	1180(70)	0.4(9)	124(32)	0.13(23)	204(38)
HD 187085	1	8.50	5.9	1032(11)	0.87(8)	24(38)	0.11(7)	120(37)					
	2	17.49	8.0	1031(14)	0.9(8)	347(62)	0.07(8)	157(50)	26.4(1.1)	0.07(13)	243(34)	0.0(3)	243(52)
HD 190228	1	0.78	7.4	1136(10)	5.9(3)	171(9)	0.53(3)	101(2)					
	2	1.11	8.4	1108(26)	7(5)	123(42)	0.17(26)	208(59)	1110(19)	7(5)	208(59)	0.20(17)	346(54)
HD 192310	1	12.51	3.3	74.4(1)	0.042(6)	249(33)	0.34(12)	22(20)					
	2	5.99	1.9	74.4(2)	0.05(1)	51(41)	0.04(14)	9(55)	629(64)	0.05(13)	285(28)	0.03(25)	25(50)
HD 196885	1	5.11	19.5	1277(13)	2.1(2)	162(12)	0.32(5)	96(12)					
	2	77.38	78.3	1343(46)	4(3)	216(82)	0.19(13)	69(24)	391(5)	3(8)	250(30)	0.2(2)	128(50)
HD 204941	1	4.26	1.3	1595(67)	0.26(4)	131(43)	0.14(9)	265(29)					
	2	3.76	1.1	1696(119)	0.23(2)	55(23)	0.07(9)	357(52)	8.31(1)	0.01(1)	270(58)	0.0(3)	0(34)
HD 210277	1	2.04	6.8	442.16(35)	1.29(5)	141(2)	0.473(12)	118(2)					
	2	6.92	8.6	443(40)	1.2(5)	358(35)	0.04(44)	91(54)	443.2(7)	2.4(5)	141(53)	0.20(9)	125(27)

Table 2—Continued

Star	Method	χ^2_ν	RMS (m s⁻¹)	P_1 (days)	$m_1 \sin i$ (M$_{\rm Jup}$)	M_1 (degrees)	e_1	ω_1 degrees	P_2 (days)	$m_2 \sin i$ (M$_{\rm Jup}$)	M_2 (degrees)	e_2	ω_2 (degrees)
HD 213240	1	4.47	10.9	872.74(96)	4.4(2)	161(1)	0.428(9)	204.4(1.3)					
	2	12.03	11.7	870(4)	4.6(2)	336(64)	0.06(3)	252(15)	870(2)	8.0(2)	131(47)	0.20(2)	257(33)
HD 216437	1	8.28	5.8	1354(5)	2.1(1)	63(4)	0.35(2)	63(4)					
	2	10.32	6.1	1342(56)	3(3)	95(47)	0.2(2)	1343(62)	312(68)	3(3)	38(36)	0.1(3)	148(50)
HD 216770	1	3.83	8.6	118.4(9)	0.64(7)	216(27)	0.38(11)	280(20)					
	2	2.37	4.4	116.7(1.7)	0.7(3)	37(73)	0.1(3)	69(27)	41.1(3)	0.3(2)	237(51)	0.0(3)	131(62)
HD 217786	1	1.77	2.7	1314.7(3.4)	13(1)	137(2)	0.385(42)	101.2(1.7)					
	2	2.68	3.0	1295	11(10)	279(1)	0.00(8)	315(62)	631(11)	1.0(7)	59(45)	0.11(8)	298(31)
HD 218566	1	8.41	3.5	225.7(4)	0.21(2)	11(17)	0.29(7)	36(18)					
	2	6.40	2.9	224.9(7)	0.20(2)	313(37)	0.05(14)	87(25)	1311(46)	0.2(4)	229(41)	0.04(26)	58(33)
HD 222582	1	1.80	3.7	572.3(7)	7.6(4)	62(2)	0.73(2)	319(1)					
	2	109.44	28.3	586	9(7)	31(42)	0.05(20)	135(31)	573(3)	14(5)	111(33)	0.2(2)	242(25)
HD 240237	1	33.61	35.5	747(16)	5.2(9)	190(19)	0.40(16)	104(25)					
	2	25.03	29.5	753(36)	5(3)	185(44)	0.0(2)	128(45)	22.49(6)	1(2)	315(37)	0.2(3)	199(61)
HIP 2247	1	10.14	4.5	655.6(6)	5.1(3)	156(1)	0.543(5)	112(2)					
	2	155.09	15.6	632(10)	6.2(3)	108(47)	0.16(10)	130(42)	75.7(1.2)	1(1)	343(28)	0.20(21)	344(42)
HIP 5158	1	9.90	10.0	352.6(7)	1.55(2)	8(8)	0.537(fixed)	253(3)					
	2	23.04	6.2	385.7(7.9)	2(3)	156(61)	0.18(17)	209(63)	401(10)	2(3)	172(42)	0.20(14)	26(63)
HIP 57050	1	13.08	9.4	41.40(2)	0.30(4)	321(18)	0.31(fixed)	238(12)					
	2	12.95	8.6	41.40(2)	0.34(5)	318(36)	0.1(1)	244(4)	28.52(6)	0.1(1)	19(53)	0.04(34)	71(47)
iota Dra	1	9.49	14.0	511.15(8)	12.7(3)	128.5(2)	0.711(4)	91.9(7)					
	2	525.35	99.7	510	14.8(5)	160(61)	0.00(6)	65(56)	267	6(5)	243(38)	0.2(2)	163(23)
GJ 649	1	11.03	4.4	602(8)	0.35(6)	195(24)	0.32(12)	7(27)					
	2	7.21	4.1	599(5)	0.31(9)	153(61)	0.07(12)	36(64)	22.36(1)	0.05(8)	2(47)	0.2(2)	346(46)
GJ 676A	1	4.03	3.7	1057(3)	4.9(3)	211(2)	0.326(9)	85.7(1.4)					
	2	6.80	4.6	1047(24)	5(1)	223(53)	0.20(4)	26(34)	1126(270)	4(1)	185(41)	0.2(1)	203(64)
14 Her	1	5.54	13.5	1754.7(4.3)	5.2(3)	328(2)	0.388(9)	23.2(1.6)					
	2	24.92	17.1	1740(696)	6(8)	290(42)	0.19(17)	115(37)	1755(917)	5(7)	2(45)	0.19(14)	278(37)
42 Dra	1	51.21	26.8	480.2(3.2)	3.7(3)	288(6)	0.51(6)	210(7)					
	2	40.68	22.0	486(9)	4.1(5)	264(20)	0.14(10)	236(55)	69.9(6)	0.5(9)	138(62)	0.11(23)	35(51)
70 Vir	1	1.63	7.7	116.686(4)	7.4(2)	339.9(7)	0.399(3)	358.9(4)					
	2	39.03	32.9	116.706(8)	8.3(4)	224(54)	0.1995(82)	355(75)	116.7(5.6)	1.7(6)	79(39)	0.1(3)	309(36)

– 20 –

[a]Single eccentric planet.

[b]Two planets, $e < 0.2$.

Table 3.   Two-Planet Fits

Star	Mass $M_\odot$	χ^2_ν	RMS $(\mathrm{m\,s^{-1}})$	P_1 (days)	$m_1 \sin i$ (M_{Jup})	a_1 (AU)	M_1 (degrees)	e_1	ω_1 degrees	P_2 (days)	$m_2 \sin i$ (M_{Jup})	a_2 (AU)	M_2 (degrees)	e_2	ω_2 (degrees)
HD 3651	0.882	5.07	6.7	62.22(5)	0.17(3)	0.295(2)	8(44)	0.06(20)	18(43)	31.08(2)	0.09(3)	0.186(2)	318(42)	0.04(20)	55(66)
HD 7449	1.05	81.96	5.7	1693(39)	1.2(2)	2.83(9)	220(65)	0.13(11)	323(64)	615(19)	0.4(2)	1.44(5)	354(32)	0.0(2)	0(46)
HD 52265	1.17	2.19	11.2	119.1(4)	1.05(4)	0.499(5)	253(57)	0.0(1)	359(54)	59.9(2)	0.35(09)	0.316(3)	303(75)	0.05(10)	358(35)
HD 65216	0.92	1.96	7.2	572.4(2.1)	1.26(4)	1.30(3)	89(51)	0.00(2)	0(41)	152.6(6)	0.17(3)	0.54(1)	237(48)	0.02(10)	0(54)
HD 85390	0.76	4.34	1.4	822(12)	0.14(1)	1.57(5)	343(57)	0.00(8)	0(49)	3700(840)	0.20(2)	4.23(9)	156(41)	0.00(7)	0(49)
HD 89744	1.558	62.54	73.2	257.8(4)	8.3(6)	0.92(1)	171(81)	0.00(1)	0(87)	85.2(1)	3.2(3)	0.440(5)	71(18)	0.00(5)	0(86)
HD 92788	1.078	5.70	11.2	326(1)	3.6(2)	0.95(1)	348(47)	0.00(11)	6(46)	162(3)	0.9(3)	0.60(1)	66(39)	0.04(21)	0(20)
HD 117618	1.069	5.74	4.6	25.807(6)	0.21(1)	0.175(2)	217(35)	0.00(8)	0(48)	318(2)	0.2(1)	0.93(1)	304(50)	0.00(26)	0(29)
GJ 649	0.54	4.19	3.2	601(6)	0.33(5)	1.14(5)	211(49)	0.2(1)	332(52)	4.4762(4)	0.030(8)	0.043(1)	334(68)	0.20(15)	334(47)
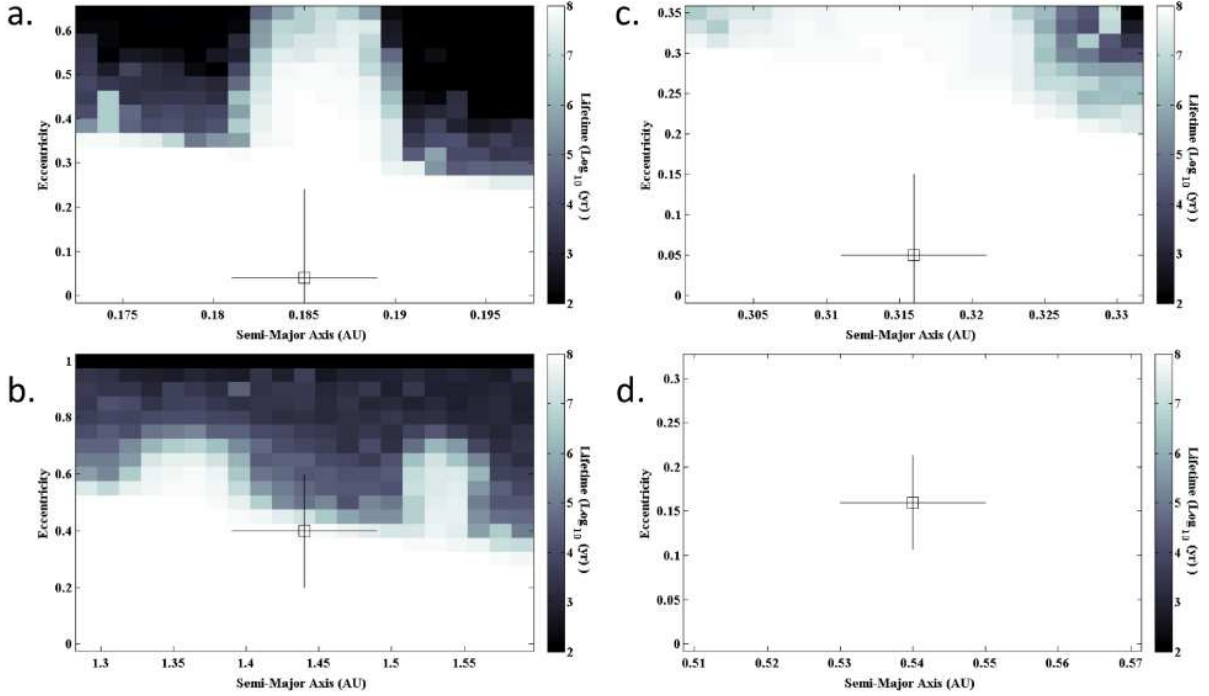
Fig. 1.— Dynamical stability for four proposed 2-planet systems, as a function of the semi-major axis, a, and eccentricity, e, of planet 2 (as given in Table 3. Ranges shown are 3σ in a and e for each system. The mean lifetime of the planetary system (in log_{10} (lifetime/yr)) at a given $a - e$ coordinate is denoted by the color of the plot. The lifetime at each $a - e$ location is the mean value of 25 separate integrations carried out on orbits at that $a - e$ position (testing a combination of 5 unique ω values, and 5 unique M values). The nominal best-fit orbit for the outer planet is shown as the small open square with $\pm$ 1-σ error bars. Panel (a): HD 3651; panel (b): HD 7449; panel (c): HD 52265; panel (d): HD 65216.
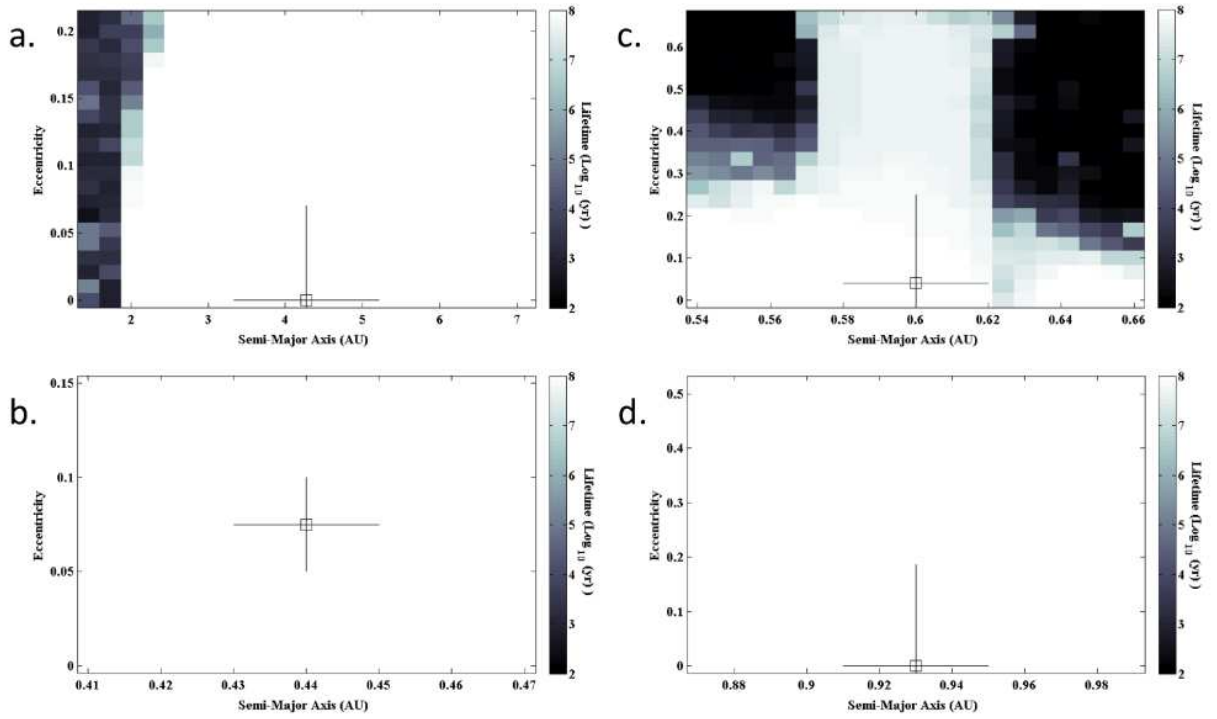
Fig. 2.— Same as Figure 1, but for the following systems: panel (a): HD 85390; panel (b): HD 89744; panel (c): HD 92788; panel (d): HD 117618.
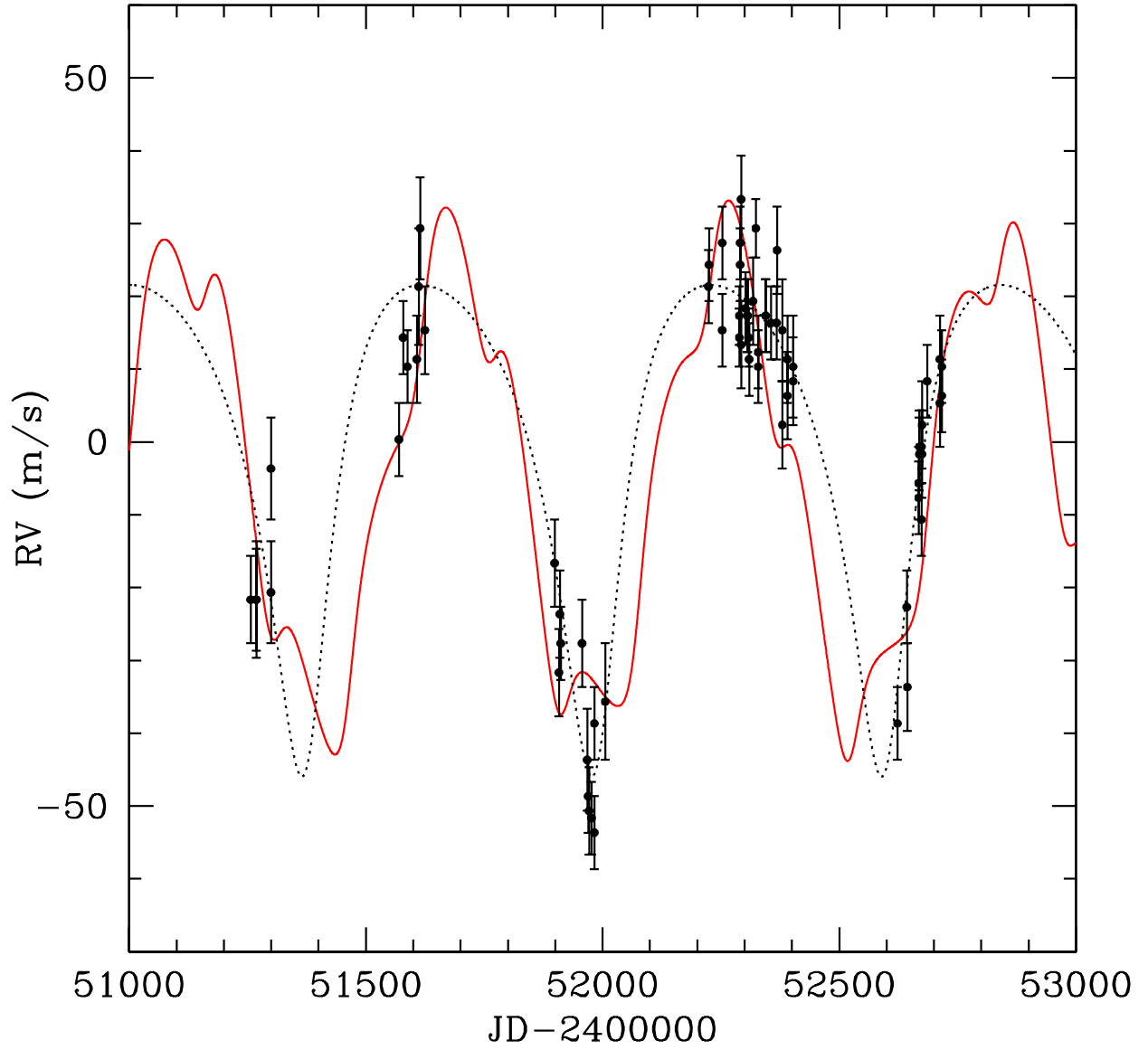
Fig. 3.— Data for HD 65216 (Mayor et al. 2004) overplotted with one-planet (dashed line) and two-planet (solid line) models. At present, the models are essentially indistinguishable, but they diverge in the future (Figure 5).
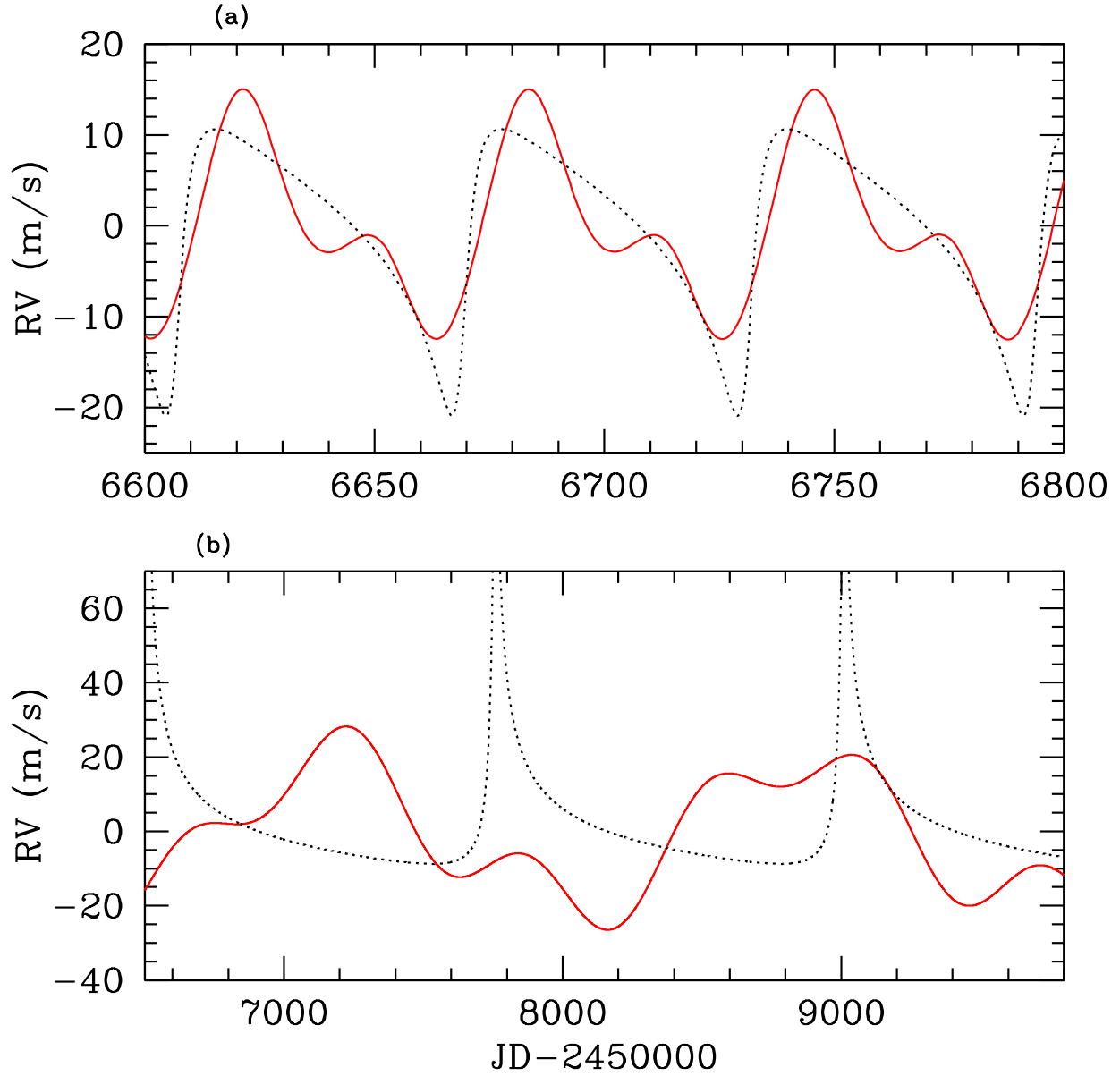
Fig. 4.— Model orbits for single and double-planet systems. In each panel, the solid (red) line is the two-planet model (Table 3), and the dashed line is the eccentric single-planet model. These plots show when in the near future the two models could be best distinguished. Panel (a)– HD 3651; panel (b)– HD 7449.
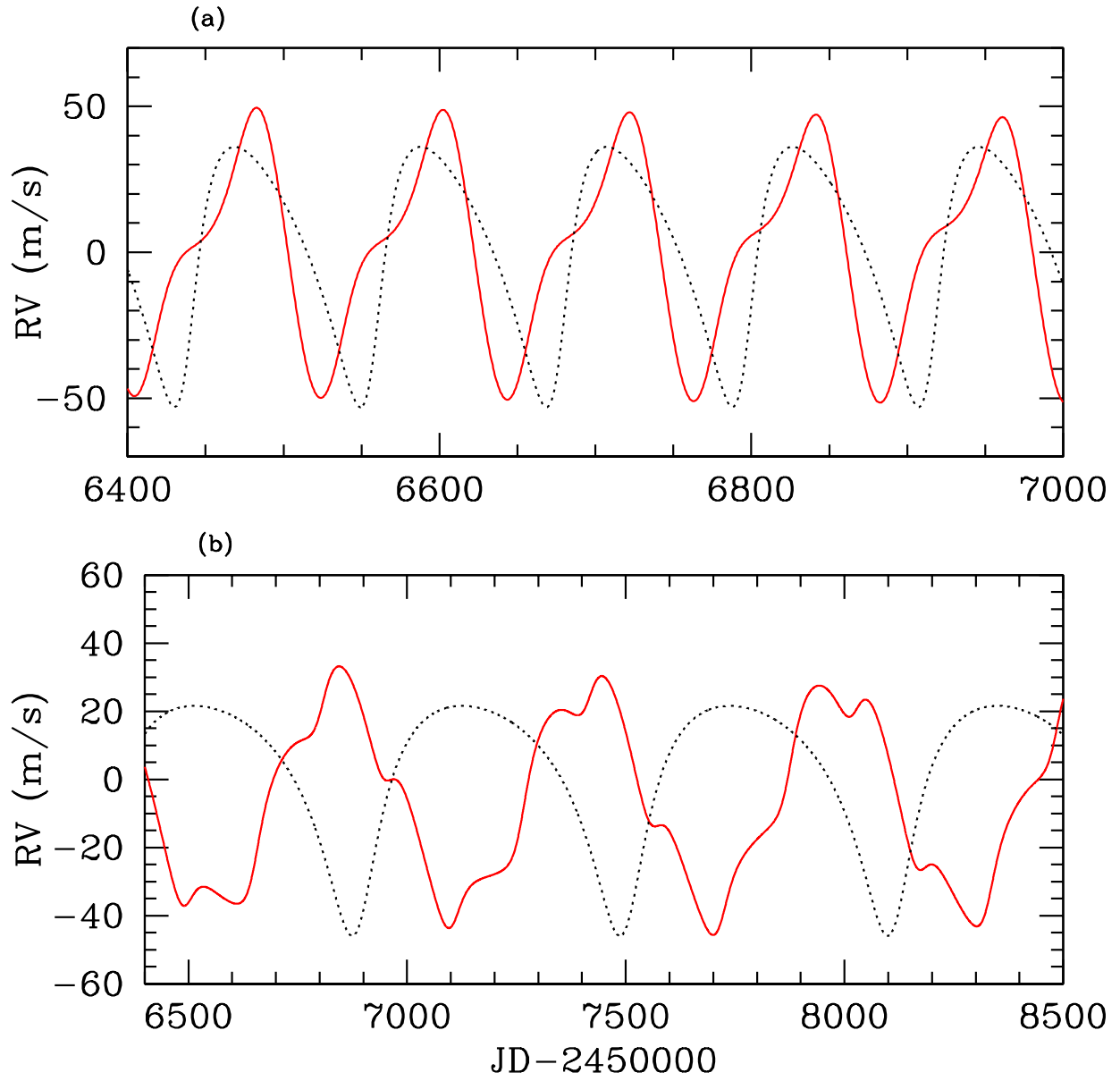
Fig. 5.— Same as Figure 4, but for the following systems: panel (a)– HD 52265; panel (b)– HD 65216.
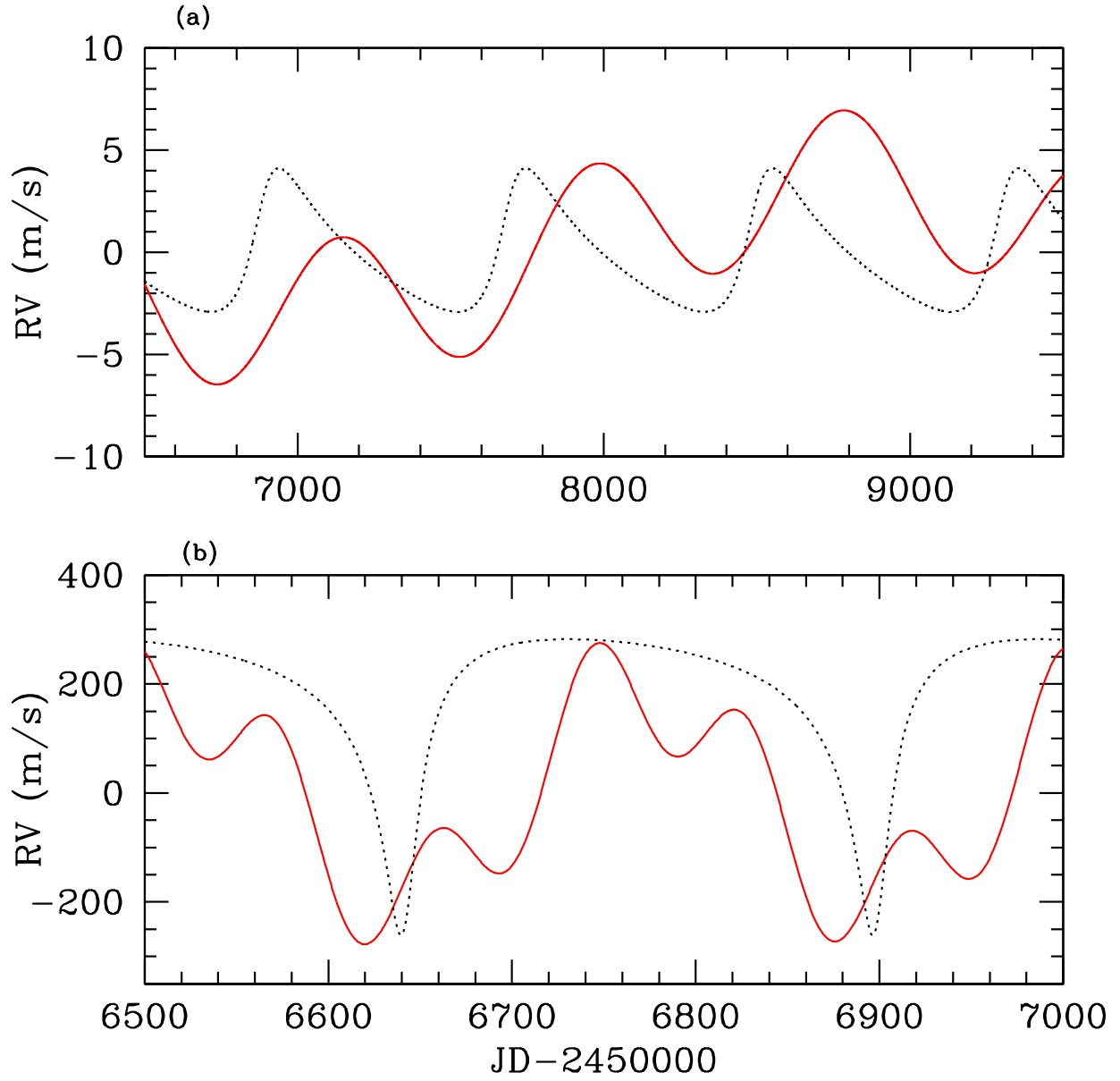
Fig. 6.— Same as Figure 4, but for the following systems: panel (a)– HD 85390; panel (b)– HD 89744.
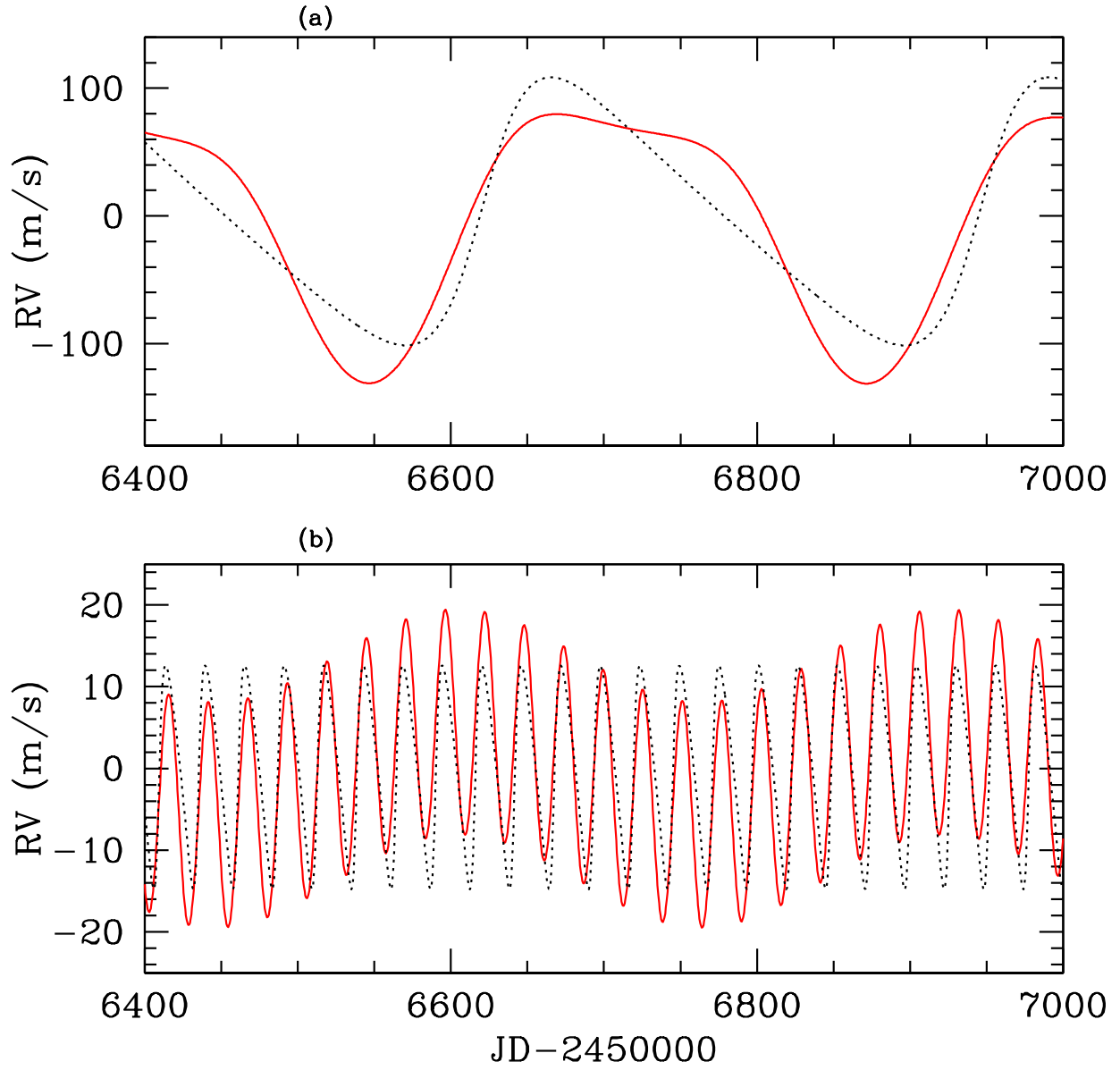
Fig. 7.— Same as Figure 4, but for the following systems: panel (a)– HD 92788; panel (b)–HD 117618.
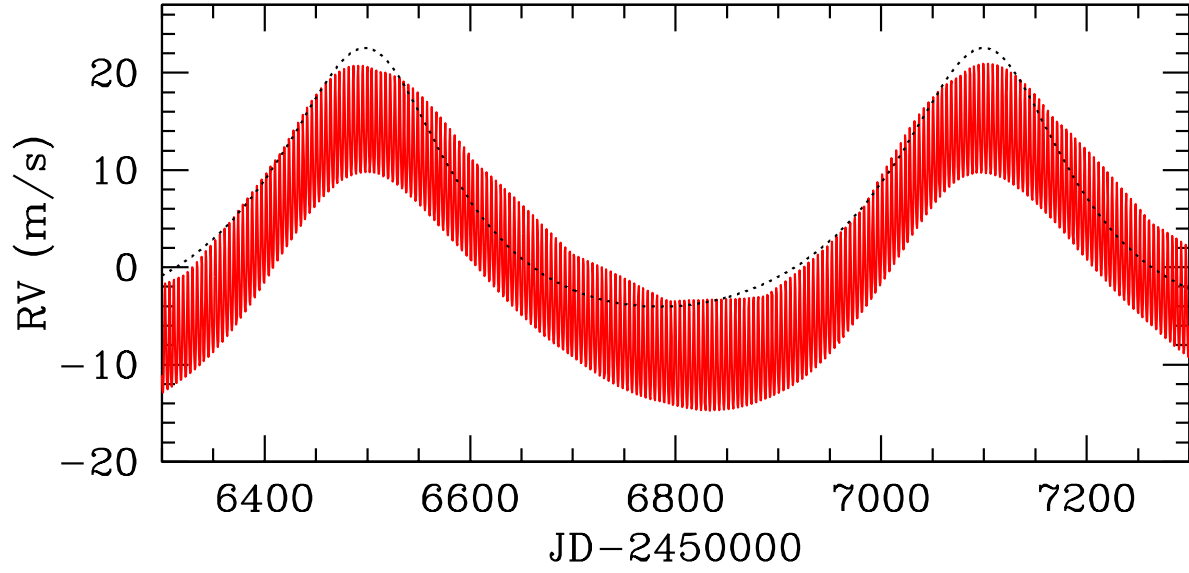
Fig. 8.— Same as Figure 4, but for GJ 649. The extremely short (4.5 day) period of the candidate second planet results in the grey region when the model velocity curve is plotted.

Table 4.   AAT Radial Velocities for HD 2039

JD-2400000	Velocity $(\mathrm{m\,s^{-1}})$	Uncertainty $(\mathrm{m\,s^{-1}})$
51118.05806	29.4	4.2
51118.96097	8.6	7.8
51119.94453	5.7	5.2
51121.03846	17.5	7.0
51211.95142	5.6	8.8
51212.92337	8.5	5.6
51213.97494	26.2	7.2
51214.91707	0.0	5.1
51386.32274	-26.6	7.6
51387.29810	-4.7	5.4
51411.22931	15.5	8.0
51414.25848	-16.2	4.7
51473.08831	-43.5	4.5
51525.92865	-53.8	8.0
51527.92257	-46.7	5.8
51745.27018	-68.7	9.9
51828.07030	-23.6	6.6
51828.99403	-34.2	5.9
51829.97574	-28.3	6.6
51856.07023	-26.5	10.3
51919.94344	-4.8	7.1
51920.96715	-8.3	6.9
52093.29473	161.2	7.0
52127.23412	104.9	7.2
52151.22296	61.7	4.4
52152.08603	68.2	3.9
52154.21237	78.9	6.0
52187.09574	62.2	4.4
52188.03000	59.2	3.6
52189.15021	55.5	5.3
52190.09323	44.7	3.4
52422.32809	-14.0	6.2
52425.33222	-15.8	3.6
52455.28482	-10.2	2.7
52511.10451	-0.5	6.6
52599.01528	-13.1	6.8
53007.02913	-6.3	2.7
53045.91967	-2.3	6.3
53245.25642	112.7	3.6
53579.22474	0.5	2.9
54013.11160	-24.1	1.9
54369.10873	79.4	2.3
55102.09594	-43.0	3.6
55430.23438	131.6	4.2
55463.19594	95.8	5.8

Table 5.   AAT Radial Velocities for HD 20782

JD-2400000	Velocity ($m\,s^{-1}$)	Uncertainty ($m\,s^{-1}$)
51035.31946	21.7	2.3
51236.93065	-6.7	3.3
51527.01731	7.1	3.4
51630.88241	29.5	2.7
51768.30885	-6.8	2.6
51828.11066	-7.8	3.0
51829.27449	-6.8	3.8
51829.99625	-26.7	8.7
51856.13530	-10.5	3.5
51919.00660	-3.8	2.9
51919.99630	-1.8	2.9
51983.89009	4.0	3.3
52092.30437	17.7	2.4
52127.26814	17.5	2.8
52152.16308	23.0	2.5
52187.15965	22.7	2.5
52511.20613	-1.4	2.3
52592.04802	17.3	2.3
52654.96031	15.2	2.4
52859.30540	-202.7	1.9
52946.13848	-18.3	2.1
52947.12256	-14.4	1.8
53004.00130	-0.5	1.9
53044.02367	0.5	2.2
53045.96101	-0.6	1.9
53217.28806	8.9	1.7
53282.22016	20.5	1.9
53398.96943	20.5	1.4
53403.96080	28.5	2.6
53576.30682	-9.4	1.6
53632.28115	-7.9	1.6
53665.18657	6.2	1.7
54013.21634	31.1	1.5
54040.13193	22.0	2.0
54153.97021	-11.6	2.1
54375.24665	13.2	1.7
54544.89156	10.0	2.1
54776.10133	-7.7	1.9
54843.02061	0.1	1.6
54899.92412	-0.8	2.1
55107.24720	16.5	2.8
55170.05454	17.1	2.4
55204.97999	29.0	1.9
55253.91182	-78.3	2.3
55399.32278	-8.4	1.9
55426.31464	-7.1	1.7

Table 5—Continued

JD-2400000	Velocity ($\mathrm{m\,s^{-1}}$)	Uncertainty ($\mathrm{m\,s^{-1}}$)
55461.23926	-15.1	3.0
55519.13337	8.2	2.0
55844.13584	-144.3	6.6
55845.17962	-187.0	2.3
55846.13670	-156.4	2.3
55964.93111	7.5	2.9

Table 6.   AAT Radial Velocities for HD 23127

JD-2400000	Velocity $(m\,s^{-1})$	Uncertainty $(m\,s^{-1})$
51118.09281	-20.9	5.2
51119.17693	-7.8	6.0
51120.26302	-65.5	8.8
51121.12041	-40.5	4.8
51157.11008	-26.3	4.2
51211.97892	-65.7	4.9
51212.95830	-37.5	4.0
51213.99302	-31.5	3.9
51214.94428	-47.4	3.3
51473.24554	21.5	5.9
51920.00758	-5.7	6.8
51983.88167	9.1	6.2
52092.31518	-0.4	4.7
52127.28906	16.5	8.4
52128.31303	17.8	8.9
52151.30892	15.4	3.4
52152.19974	0.0	3.9
52188.15301	5.3	3.1
52189.16917	-3.3	4.5
52477.33581	-47.6	11.2
52595.09050	-5.2	5.2
52655.03366	-3.7	5.0
52947.13705	16.2	2.0
53004.02539	20.3	1.6
53045.99621	11.0	2.3
53217.30387	1.3	2.3
53281.22070	-1.4	2.0
53577.31797	-34.3	2.5
53628.28608	-38.7	2.6
53632.25573	-43.6	3.8
53669.20119	-39.2	2.2
53944.33250	2.7	1.9
54010.19795	6.2	1.8
54037.14466	4.0	2.1
54374.24189	11.2	1.7
54432.04206	31.4	4.3
54552.89944	-3.1	2.8
54905.91119	-37.7	2.8
55105.20438	-16.3	2.9
55172.05265	13.0	2.4
55430.30950	21.1	2.9
55522.11944	32.9	3.0
55524.10270	18.4	8.9
55967.93302	-4.9	3.4

Table 7.   AAT Radial Velocities for HD 38283

JD-2400000	Velocity ($m\,s^{-1}$)	Uncertainty ($m\,s^{-1}$)
50829.98715	-4.1	1.6
50831.11229	-0.3	1.6
51157.14186	-22.1	2.3
51213.00749	3.1	2.6
51526.07541	-16.5	2.6
51530.13214	-7.4	3.0
51683.84877	6.7	2.4
51921.13329	6.0	1.9
52188.26174	-4.4	2.4
52594.17205	-8.1	2.2
52654.09309	6.7	2.3
52751.89940	4.2	2.1
53004.05785	-6.7	1.6
53042.04257	1.4	2.1
53043.01088	-3.5	2.1
53044.05527	-1.0	2.3
53047.04258	5.5	1.9
53048.08703	0.8	1.9
53214.31960	-2.8	1.9
53283.27433	-6.4	2.5
53399.05143	4.5	1.6
53483.85275	10.2	1.8
53484.86059	4.2	1.7
53486.87865	4.1	1.8
53487.88987	3.9	1.7
53842.85825	6.8	1.3
54011.27866	-4.6	1.8
54018.25770	-10.8	2.2
54037.19283	-6.8	2.7
54038.22781	-18.4	2.3
54040.19869	-16.3	2.6
54118.99517	0.1	1.4
54221.85332	5.8	1.4
54371.28261	-1.9	1.6
54432.16897	-11.7	2.7
54545.96278	4.5	1.6
54777.16327	-18.1	2.4
54780.22622	-7.9	1.6
54899.97099	-1.3	2.4
55105.27655	-10.2	2.3
55171.10597	-5.7	1.7
55201.13167	-7.4	2.1
55205.04258	3.0	1.7
55252.94918	10.7	1.7
55309.87992	11.9	1.4
55312.85776	15.3	1.9

Table 7—Continued

JD-2400000	Velocity ($\mathrm{m\,s^{-1}}$)	Uncertainty ($\mathrm{m\,s^{-1}}$)
55315.85591	8.7	1.5
55376.33979	-0.6	1.6
55377.34088	1.8	1.9
55398.31564	-8.5	1.3
55401.33166	-9.2	1.6
55457.28957	-4.9	2.0
55462.26265	-5.7	2.2
55519.20219	-2.7	1.9
55524.14501	0.4	1.7
55603.01744	8.8	1.9
55665.89491	10.8	2.3
55691.88048	23.2	1.7
55874.20082	-12.4	2.1
55898.15704	-2.5	2.3
55963.02880	15.8	2.0

Table 8.   AAT Radial Velocities for HD 39091

JD-2400000	Velocity ($\mathrm{m\,s^{-1}}$)	Uncertainty ($\mathrm{m\,s^{-1}}$)
50829.99300	0.3	2.2
51119.25037	-29.4	4.6
51236.03289	-38.2	2.7
51411.32492	-41.8	2.8
51473.26697	-39.2	2.2
51526.08042	-51.0	2.2
51527.08206	-47.4	2.0
51530.12796	-45.8	2.2
51629.91162	-50.3	2.5
51683.84224	-56.4	2.3
51828.18751	-24.3	2.1
51919.09891	2.8	3.3
51921.13833	-0.4	2.3
51983.91910	34.0	2.4
52060.83961	178.8	2.1
52092.33661	252.8	2.2
52093.35148	253.3	2.0
52127.32781	327.6	2.7
52128.33566	327.9	2.0
52130.33830	330.0	3.1
52151.29169	349.2	2.2
52154.30426	338.8	5.0
52187.19587	325.7	1.8
52188.23586	326.7	1.9
52189.22191	320.9	1.7
52190.14484	320.9	1.9
52387.87064	140.3	1.7
52510.30664	83.2	2.1
52592.12558	59.7	1.5
52599.15463	59.4	5.7
52654.09858	56.8	2.3
52708.98434	42.3	11.4
52751.91773	29.8	2.1
52944.22372	-1.5	1.9
53004.07471	6.9	1.9
53042.07800	-0.5	2.0
53043.01734	-3.6	2.2
53047.04936	0.0	2.1
53048.09782	-6.3	1.7
53245.31090	-29.2	2.5
53402.03480	-21.7	0.9
53669.24365	-44.6	1.0
54012.24920	8.2	0.9
54039.16869	16.9	1.1
54224.85303	339.5	1.1
54336.31438	246.9	1.8

Table 8—Continued

JD-2400000	Velocity ($\mathrm{m\,s^{-1}}$)	Uncertainty ($\mathrm{m\,s^{-1}}$)
54337.29175	251.3	1.6
54372.27038	208.0	1.8
54425.22432	171.5	1.3
54545.94257	104.4	1.1
54841.06346	33.9	1.4
54901.94078	19.7	2.0
54905.99137	18.0	1.6
54906.97424	18.5	1.3
55106.23926	-4.7	1.9
55170.23742	-6.3	1.3
55202.05426	-1.5	1.9
55252.96918	-19.1	1.4
55521.20064	-32.6	1.6
55585.99614	-23.1	1.7
55664.85733	-31.0	1.5
55846.25128	-35.0	1.5
55898.10923	-34.1	1.3
55899.13681	-35.7	1.4
55962.00315	-23.3	1.3
55965.03864	-24.6	1.4
55966.97920	-22.9	2.3

Table 9.   AAT Radial Velocities for HD 102365

JD-2400000	Velocity $(\mathrm{m\,s^{-1}})$	Uncertainty $(\mathrm{m\,s^{-1}})$
50830.21201	-2.2	1.5
50970.88818	0.2	1.2
51213.22626	-7.9	1.4
51236.20861	4.1	3.4
51237.10884	-4.7	2.1
51274.16691	-1.8	1.3
51275.06855	-10.8	2.2
51382.90174	-6.6	1.4
51631.04270	-5.4	1.4
51682.83774	-4.7	1.7
51684.05028	1.0	1.5
51717.85402	-3.6	1.5
51743.86802	-2.0	1.5
51919.23487	0.2	2.4
51984.12770	-6.5	1.8
52009.15814	0.0	1.4
52060.92662	-1.6	1.5
52127.86705	-3.8	2.0
52388.04297	-7.1	1.5
52420.97249	2.8	1.5
52421.97640	1.6	1.5
52422.90505	-0.8	1.6
52423.97700	-0.5	1.8
52424.97954	-1.0	1.1
52455.88825	-7.4	1.5
52654.27164	1.8	1.6
52745.02160	-3.9	1.6
52749.07992	-2.9	1.6
52751.07418	1.0	1.6
52783.96280	1.1	1.7
52860.84417	3.7	1.6
53005.25313	5.9	2.0
53008.21509	1.7	1.6
53041.28500	2.4	1.5
53042.21355	0.2	1.5
53048.25853	1.9	1.6
53051.18853	5.3	1.5
53214.87086	0.1	1.6
53245.85116	-0.3	2.2
53402.19479	0.2	0.8
53482.94177	3.5	0.9
53483.97344	-2.1	0.9
53485.00857	-0.8	0.8
53485.92867	-2.6	0.9
53486.99104	-2.9	0.8
53488.05937	-4.2	0.8

Table 9—Continued

JD-2400000	Velocity $(\mathrm{m\,s^{-1}})$	Uncertainty $(\mathrm{m\,s^{-1}})$
53488.97513	-2.5	0.8
53506.91912	2.5	0.9
53509.01692	0.2	0.9
53509.84592	-2.9	0.8
53515.85480	4.0	0.8
53516.84760	4.4	0.9
53517.87645	2.0	0.8
53518.93476	2.6	0.8
53519.83473	2.5	0.9
53520.97000	1.9	0.9
53521.91817	-1.1	0.9
53522.95210	0.4	0.9
53568.84360	-3.6	0.8
53569.86061	-2.1	0.9
53570.88393	-4.4	0.9
53571.89292	-5.1	0.9
53572.86541	-1.6	0.9
53573.84968	-4.2	0.8
53575.85410	-1.2	0.8
53576.85102	-1.8	0.8
53577.84683	-1.5	0.8
53578.84583	-0.2	0.8
53700.24588	0.4	0.9
53753.24814	0.1	1.1
53840.11811	-7.6	1.2
53841.00289	-1.4	0.8
53844.01699	-1.1	0.9
53937.87450	0.0	0.8
54038.24696	-2.3	1.3
54111.18437	4.2	0.9
54112.19360	2.5	0.7
54113.21647	3.4	0.9
54114.22365	2.2	0.8
54115.22923	1.0	1.1
54119.23118	2.3	0.8
54120.17724	-0.5	0.7
54121.18308	-0.2	0.7
54123.20774	2.9	0.7
54126.14491	-1.8	0.7
54127.15427	3.0	0.6
54128.16856	0.7	0.9
54129.17063	-1.2	0.6
54130.16450	2.4	0.7
54131.17111	1.7	0.7
54132.17838	0.1	0.9
54133.24020	2.0	1.0

Table 9—Continued

JD-2400000	Velocity (m s^{-1})	Uncertainty (m s^{-1})
54134.20214	0.3	1.0
54135.16844	2.3	0.8
54136.18672	1.7	0.8
54137.18488	2.0	0.7
54138.16588	0.1	1.1
54139.15652	1.9	0.8
54140.15870	3.2	0.9
54141.18313	3.9	0.9
54142.17798	2.1	0.6
54144.06348	1.3	0.7
54145.14432	2.2	0.8
54146.14936	0.7	0.7
54147.18172	-1.0	0.7
54148.21150	-1.0	0.8
54149.15042	-2.1	0.8
54150.14582	-1.9	0.7
54151.19287	-1.9	0.7
54152.20783	-0.2	0.9
54153.15877	-3.6	0.9
54154.10999	-3.0	0.6
54155.07901	-1.9	0.7
54156.05374	-2.5	1.1
54222.04514	-1.5	1.7
54223.06951	2.5	1.0
54224.08922	0.6	0.9
54225.03639	-1.9	0.8
54226.00289	-2.1	1.3
54252.95650	-0.1	0.9
54254.90643	1.8	1.0
54255.92803	-3.5	1.0
54257.05236	-4.5	1.1
54543.11240	-3.2	0.8
54550.07875	0.1	1.4
54551.04141	-2.4	1.0
54553.06907	-6.7	1.1
54841.22838	2.6	1.1
54843.26009	0.2	1.1
54897.14254	0.7	1.0
54901.13378	-3.1	1.1
54902.14792	-0.8	1.1
54904.17743	-7.3	1.4
54905.17801	-6.5	0.9
54906.19747	-4.1	1.1
54908.17853	-6.3	1.0
55031.89041	-4.5	0.9
55202.19583	6.7	1.2

Table 9—Continued

JD-2400000	Velocity $(\mathrm{m\,s^{-1}})$	Uncertainty $(\mathrm{m\,s^{-1}})$
55204.23690	1.6	1.4
55206.17590	0.3	1.0
55231.14629	2.7	1.1
55253.16083	2.9	1.0
55310.04537	-2.6	1.2
55312.05141	-2.7	1.0
55313.06557	3.6	1.1
55314.97472	-3.4	1.0
55316.99125	-3.3	1.1
55370.88444	1.1	1.2
55371.88362	-6.5	1.0
55374.93147	4.5	1.5
55376.86882	-2.7	1.2
55397.85721	-4.6	1.1
55398.85407	-4.8	0.9
55586.17916	8.4	1.1
55603.28296	12.5	1.4
55604.09249	8.6	0.9
55664.07027	9.6	1.0
55666.02599	1.2	1.0
55692.02182	12.0	1.2
55692.99384	8.4	1.1
55750.86140	4.1	1.1
55751.84824	9.1	2.2
55753.83346	7.7	1.0
55756.86016	5.2	1.6
55785.87243	-0.7	1.3
55787.84349	10.7	1.2
55878.26267	-1.7	2.7
55961.14964	11.2	1.0

Table 10.   AAT Radial Velocities for HD 108147

JD-2400000	Velocity ($m\,s^{-1}$)	Uncertainty ($m\,s^{-1}$)
50830.24279	26.4	2.6
50915.04863	-7.8	4.0
51213.25018	10.1	4.4
51276.06356	21.0	4.3
51382.88648	-43.0	2.5
51631.05277	-28.9	2.6
51682.96554	-6.1	2.7
51718.00741	-10.1	2.8
51856.26359	16.1	4.7
51984.09097	34.3	4.0
52009.12841	-7.8	3.0
52010.19667	-25.6	2.9
52061.02192	38.4	2.8
52091.89265	0.2	2.8
52126.88255	-19.0	9.5
52127.87323	0.8	3.1
52129.89531	-6.9	2.9
52360.17918	-13.8	3.6
52387.01113	-4.5	2.1
52388.03800	21.6	2.1
52389.03674	9.8	2.3
52390.02488	0.7	2.3
52420.97941	30.1	2.2
52421.99109	17.2	2.3
52423.06610	1.9	2.4
52423.98213	9.0	2.5
52424.98647	-5.5	2.6
52452.95259	18.1	3.3
52454.90924	0.2	2.7
52455.90437	4.5	2.9
52509.85414	5.2	2.2
52510.85405	-5.2	2.4
52598.25801	46.1	6.5
52599.25428	40.1	7.4
52654.25245	-16.0	3.0
52655.17027	-12.7	3.1
52710.11861	-21.0	4.2
52710.93403	-16.3	4.1
52712.05281	-21.7	3.8
52745.08065	-34.3	2.9
52746.05949	-12.0	3.1
52748.02643	29.3	2.5
52749.08757	6.0	2.7
52750.03644	-12.7	2.7
52751.08725	-11.5	2.6
52752.04493	-13.0	2.6

Table 10—Continued

JD-2400000	Velocity ($m\,s^{-1}$)	Uncertainty ($m\,s^{-1}$)
52783.95060	10.7	2.0
52785.05259	1.1	2.6
52785.97642	-17.7	2.6
52857.86852	15.8	2.7
52858.87366	-2.2	2.7
52859.85266	3.6	3.2
52860.85516	0.0	2.5
53516.99066	-2.5	3.5
54899.12290	-12.7	4.1
55962.19009	-9.6	3.4
55996.08993	45.3	3.3

Table 11.   AAT Radial Velocities for HD 117618

JD-2400000	Velocity ($\mathrm{m\,s^{-1}}$)	Uncertainty ($\mathrm{m\,s^{-1}}$)
50831.18597	-10.3	2.4
50917.10104	10.1	3.6
50970.94927	17.1	2.8
51212.20608	-12.2	3.1
51236.22669	2.8	6.7
51274.24419	0.6	3.7
51383.93108	2.7	2.5
51386.85838	3.1	2.5
51631.25935	-28.3	2.4
51682.97674	-15.0	2.8
51718.03450	4.3	2.9
51920.26309	6.2	3.4
51984.10352	-17.1	4.2
52092.96337	-15.1	2.5
52129.00532	5.0	4.2
52387.04015	8.4	1.9
52388.07932	11.9	2.2
52422.00889	-0.3	2.0
52452.97667	-10.6	1.9
52455.92575	-4.3	2.1
52509.87274	-13.7	1.9
52510.87230	-6.2	2.0
52710.17758	-8.6	1.8
52710.96784	-4.1	2.0
52712.07590	-10.6	1.8
52745.14346	11.4	2.3
52750.10349	14.2	1.8
52752.08891	13.0	1.9
52784.00059	2.6	3.1
52785.06453	-3.7	1.7
52785.98821	-6.8	1.8
52857.88042	12.0	1.7
53006.24282	7.1	1.8
53007.24111	1.1	2.4
53008.23805	12.6	1.6
53041.23361	7.6	2.6
53042.22925	-4.9	1.8
53044.16694	-9.1	2.2
53045.27837	-11.9	2.1
53046.08722	-12.0	2.3
53046.27982	-10.5	2.7
53047.20181	-15.0	1.8
53051.19446	-10.6	1.9
53213.99332	9.6	1.5
53214.89437	8.3	1.6
53215.89127	9.0	1.9

Table 11—Continued

JD-2400000	Velocity $(\mathrm{m\,s^{-1}})$	Uncertainty $(\mathrm{m\,s^{-1}})$
53216.92640	8.2	1.8
53242.90299	3.0	1.7
53244.94716	3.8	2.2
53245.88103	5.1	1.8
53399.20905	11.4	1.5
53405.21458	-5.6	1.5
53483.04532	-12.1	2.5
53485.09022	-8.7	1.9
53507.02859	-1.6	1.9
53521.98706	13.9	1.7
53568.94925	-9.3	1.7
53576.90329	-1.1	1.5
53943.90016	-5.1	1.3
54144.17378	9.5	1.8
54224.16387	2.6	1.8
54254.02748	-1.5	1.6
54545.13700	-25.7	1.5
54897.21961	10.0	1.9
54904.21623	-18.7	3.0
55313.10430	1.2	1.6
55376.93152	1.8	1.7
55402.89503	-6.5	1.8
55665.16541	23.3	1.7
55964.26135	-1.9	1.6

Table 12.   AAT Radial Velocities for HD 142415

JD-2400000	Velocity ($m\,s^{-1}$)	Uncertainty ($m\,s^{-1}$)
52390.12777	29.8	1.8
52422.09531	24.7	1.6
52425.10054	4.3	2.0
52453.01048	-4.2	2.3
52476.98791	9.2	2.3
52745.18623	14.5	2.6
52751.17456	15.1	2.5
52858.91808	12.6	2.4
53486.12760	-97.2	2.4
53509.16629	-9.1	2.0
53520.12129	2.3	3.0
53576.98888	33.9	2.5
53844.17161	-37.3	1.6
53944.98514	11.3	1.7
54226.07632	0.0	1.6
54256.02792	-40.8	2.9
54373.88492	78.9	2.2
54544.25079	44.1	1.8
55020.87803	-21.1	2.3
55043.95806	-32.6	1.6
55054.91417	-34.8	1.5
55076.98252	-58.2	2.2

Table 13.   AAT Radial Velocities for HD 187085

JD-2400000	Velocity ($\mathrm{m\,s^{-1}}$)	Uncertainty ($\mathrm{m\,s^{-1}}$)
51120.91699	-14.0	2.5
51411.07528	1.8	3.4
51683.16928	22.4	2.9
51743.04943	15.8	3.0
51767.00464	13.7	2.4
51769.06523	4.7	2.2
51770.11535	11.7	2.6
51855.94773	7.1	4.3
52061.21399	-2.2	2.6
52092.05117	-24.1	2.9
52128.02674	-18.8	2.5
52151.01458	-10.6	3.2
52189.92296	-8.4	2.0
52360.28155	-6.1	2.5
52387.21676	-9.1	1.9
52388.23551	-10.7	2.1
52389.26643	-12.9	2.3
52422.21212	-3.1	2.2
52456.09167	-6.0	2.5
52750.25882	11.8	1.9
52752.23100	13.6	2.0
52784.20681	23.0	1.8
52857.12186	3.5	1.9
52861.01669	16.4	2.3
52942.98422	17.3	2.2
52946.92563	18.9	1.8
53217.06633	-9.0	2.0
53245.04289	-21.2	2.8
53484.30018	-1.5	1.9
53489.26010	-6.6	1.7
53507.19655	2.2	1.4
53510.21563	-2.6	1.8
53517.26209	-2.5	2.2
53520.27478	-4.6	2.2
53569.08540	0.1	2.0
53572.16686	-3.2	2.2
53577.02722	6.2	1.6
53627.96289	14.7	3.2
53632.07459	10.7	1.7
53665.95368	20.3	1.9
53945.13814	11.3	1.4
54008.96665	8.3	1.6
54016.93647	4.8	1.7
54225.29248	-19.5	2.0
54254.14742	-8.7	1.8
54338.14695	-15.1	1.7

Table 13—Continued

JD-2400000	Velocity $(\mathrm{m\,s^{-1}})$	Uncertainty $(\mathrm{m\,s^{-1}})$
54371.96418	-4.0	1.6
54544.28035	-11.0	1.9
54779.95738	11.3	2.1
55101.98352	8.3	1.8
55105.98996	-8.0	2.4
55109.00947	3.6	1.8
55110.96110	3.8	2.3
55111.95166	3.9	1.6
55313.29333	-18.6	1.6
55315.24843	-17.4	1.8
55317.23004	-17.8	2.1
55376.17401	-16.9	1.9
55399.11015	-16.1	2.3
55430.02150	-3.9	2.1
55462.01469	-1.7	2.7
55664.31796	12.3	1.7
55755.04339	11.1	1.9
55844.91980	33.1	2.4

Table 14.   AAT Radial Velocities for HD 213240

JD-2400000	Velocity ($m\,s^{-1}$)	Uncertainty ($m\,s^{-1}$)
51034.19977	45.8	2.0
51119.03196	19.7	5.0
51683.29093	23.0	2.1
51745.21846	43.6	2.3
51767.18008	45.3	1.8
51768.20681	43.2	2.3
51856.03358	44.1	3.1
51856.90638	48.4	4.9
52010.31187	23.8	2.1
52062.32344	14.9	1.9
52092.20773	15.4	2.1
52093.21992	0.0	2.0
52127.17837	6.5	2.3
52151.12818	-6.9	1.9
52186.94703	-23.2	1.5
52188.04540	-20.9	2.1
52189.03997	-22.8	1.1
52189.96724	-25.8	1.5
52388.30013	-133.9	1.8
52389.30681	-137.5	3.2
52421.33402	-99.2	1.7
52423.30063	-95.0	1.8
52425.31971	-91.5	1.6
52477.19309	-24.4	2.1
52511.01295	12.8	2.0
52593.94991	31.5	3.4
52861.16704	34.1	2.2
53216.25264	-133.0	2.0
53244.17584	-145.3	1.9
53576.18990	45.9	1.6
54013.02040	-73.8	1.2
54256.22716	9.2	1.5
54776.91931	-23.0	1.9
55102.03566	-19.1	1.6
55520.94864	36.3	1.9

Table 15.   AAT Radial Velocities for HD 216437

JD-2400000	Velocity $(\mathrm{m\,s^{-1}})$	Uncertainty $(\mathrm{m\,s^{-1}})$
50830.94196	-16.0	1.6
51034.22506	-16.3	1.8
51386.30509	10.0	2.2
51472.95520	20.2	1.8
51683.31464	49.4	1.9
51684.32758	48.7	1.8
51743.23428	61.1	2.9
51767.20463	58.8	1.7
51768.22482	54.0	1.9
51828.04269	65.4	2.0
51828.96337	56.3	2.0
51829.95683	55.0	2.1
51856.04780	48.6	3.7
51919.92935	47.8	1.8
51920.92549	50.4	2.1
52061.28844	-2.5	2.0
52092.22059	-5.6	1.9
52127.19806	-3.5	2.2
52154.10649	-17.0	2.0
52188.08067	-31.4	1.4
52387.31939	-6.7	1.7
52388.30982	-8.7	1.0
52389.29622	-12.9	3.1
52390.31831	-13.2	2.1
52422.30856	-15.1	1.7
52425.32603	-11.6	1.6
52456.28016	-10.9	2.0
52477.20241	-9.0	2.2
52511.03790	-5.5	1.9
52594.93793	-1.8	1.5
52861.20216	32.8	2.2
52945.03284	36.5	2.0
53006.97127	44.8	1.9
53215.25326	56.1	1.4
53244.19252	52.5	2.2
53509.30457	-9.1	0.9
53523.32674	-18.2	1.2
53577.20037	-21.6	0.9
53632.15021	-24.1	0.9
53943.23990	0.3	0.7
54012.06760	2.7	0.8
54014.10754	3.2	1.1
54255.20770	26.3	1.1
54375.09160	39.1	0.9
54427.02974	43.6	3.2
54752.04756	0.1	0.8

Table 15—Continued

JD-2400000	Velocity ($\mathrm{m\,s^{-1}}$)	Uncertainty ($\mathrm{m\,s^{-1}}$)
55106.11746	-25.4	1.3
55171.99939	-12.1	1.3
55523.92910	22.3	1.0
55751.28024	45.5	2.0